KTH Chemical Science
and Engineering

Bulk and interfacial properties of cellulose ethers

Rasmus Bodvik

Doctoral Thesis at the Royal Institute of Technology

Stockholm 2012

Akademisk avhandling som med tillstånd av Kungliga Tekniska Högskolan framläggs till offentlig granskning för avläggande av teknologie doktorsexamen fredag 1 juni 2012 klockan 10.00 i hörsal D3, Kungliga Tekniska Högskolan, Lindstedtsvägen 5, Stockholm

Rasmus Bodvik, *Bulk and interfacial properties of cellulose ethers*

TRITA-CHE Report 2012:22

ISSN 1654-1081

ISBN 978-91-7501-347-3

KTH, Royal Institute of Technology

Department of Chemistry, Surface and Corrosion Science

Drottning Kristinas väg 51

SE-100 44 Stockholm

Sweden

Abstract

This work summarizes several studies that all concern cellulose ethers of the types methylcellulose (MC) hydroxypropylmethylcellulose (HPMC) and ethyl(hydroxyethyl)cellulose (EHEC). They share the feature of negative temperature response, as they are soluble in water at room temperature but phase separate and sometimes form gels at high temperatures. The different types of viscosity transitions occurring in these three cellulose ethers are well-known. However, earlier studies have not solved the problem of why both HPMC and EHEC, as the temperature increases, exhibit a viscosity decrease just before the viscosity increases, whereas MC only has one transition temperature where the viscosity increases. With our investigations we have aimed to compare the effect of temperature on bulk solutions and on adsorbed layers of the different polymers using a range of techniques.

Light scattering and cryo transmission electron microscopy (cryo-TEM) was employed to study aggregation of MC, HPMC and EHEC in solution. The solvent quality of water is reduced for all three polymers in solution as the temperature increases, and this infers an onset of aggregation at a certain temperature. The aggregation rate follows the order EHEC > HPMC > MC. Cryo-TEM pictures of solutions frozen from high temperatures showed closely packed fibrils forming dense networks in MC solution. Some fibrils were also found in HPMC solution above the transition temperature, but they did not interconnect readily. This is explained by the bulky and hydrophilic hydroxypropyl groups attached to HPMC. EHEC has similar substituents, while MC only has short and hydrophobic methyl groups attached to the main chain.

An amphiphilic liquid, diethyleneglycolmonobutylether (BDG) was used as an additive to change the properties of MC solutions in water. With 10 wt% BDG added, the effect was similar in viscosity and light scattering measurements as well as cryo-TEM pictures, inducing a temperature response resembling that of HPMC in pure water. 5 wt% of BDG was enough to change the aggregation type and induce a transition temperature with viscosity decrease. The effect of the additive is rationalized by BDG acting as a hydrophobic and bulky substituent in MC, similar to the large substituents in HPMC and EHEC.

Two instruments, a quartz crystal microbalance with dissipation (QCM-D) and an ellipsometer, were used in parallel to determine the changes with temperature on an adsorbed layer of MC and HPMC on silica kept in water and in polymer solution. The silica needed to be hydrophobized for significant adsorption to take place. Adsorption was similar for both polymers at low temperatures, whereas a sharp transition in several layer properties occurred for HPMC, but not for MC, close to the solution viscosity transition temperature. Atomic force microscopy (AFM) was used to measure attractive and repulsive forces and also friction forces between MC layers in polymer solution. The small changes in normal forces with temperature infer that the hydrophobic groups in MC are mostly depleted from the surface. The surface–polymer interactions increase with increasing temperature and the layer becomes more cohesive, which induces a higher load bearing capacity and lower friction when measured at high loads. AFM imaging was employed to obtain the height distribution in MC adsorbed layers. These images indicate that fibril-like structures were formed at a lower temperature in the surface layer than in bulk solution.

The different preferences for adsorption and for aggregation in MC and HPMC above the solution transition temperatures are explained by the fibril formation in MC shielding hydrophobic parts of the polymer from the solution, and thus counteracting adsorption, but also fast aggregation. The viscosity decrease in HPMC and EHEC is conferred to intra-chain contraction and aggregation into less extended structures.

Sammanfattning

I det här arbetet sammanfattas ett antal studier som berör cellulosaetrar av olika slag: metylcellulosa (MC), hydroxypropylmetylcellulosa (HPMC) och etyl(hydroxyetyl)cellulosa (EHEC). En gemensam egenskap för dessa tre är negativ temperaturrespons, vilket innebär att de är lösliga i vatten vid rumstemperatur men fasseparerar och ibland bildar geler vid höga temperaturer. De olika typerna av viskositetsövergångar som sker i de nämnda cellulosaetrarna är välkända. Tidigare studier har dock inte lyckats förklara varför HPMC och EHEC båda uppvisar en nedgång i viskositet just före den viskositetsuppgång som sker när temperaturen ökar, medan MC endast uppvisar en övergångstemperatur kopplad till viskositetsuppgång. Våra undersökningar har syftat till att jämföra temperaturens påverkan på bulklösningar och adsorberade lager av de olika polymererna med hjälp av flera olika tekniker.

Ljusspridning och kryotransmissionselektronmikroskopi (kryo-TEM) användes för att studera aggregeringen hos MC, HPMC och EHEC i lösning. När temperaturen ökade minskade lösningsmedelskvaliteten hos vatten för alla tre polymer vilket medförde att aggregering började vid en viss temperatur. Aggregeringshastigheten följer ordningen EHEC > HPMC > MC. Kryo-TEM-bilder av lösningar som hade frusits från höga temperaturer visade att tätt packade fibriller formas och bildar finmaskiga nätverk i MC-lösning. En del fibriller återfanns också i HPMC-lösning ovanför övergångstemperaturen men de var inte lika benägna att sammankopplas. Detta låter sig förklaras av de skrymmande och hydrofila hydroxypropylgrupperna som är fästa vid HPMC. EHEC har liknande substituenter, medan MC bara har korta och hydrofoba metylgrupper fästa vid huvudkedjan.

En amfifil vätska, dietylenglykolmonobutyleter (BDG) användes som additiv för att förändra egenskaperna hos MC-lösningar i vatten. Med en tillsats av 10 vikts-% BDG åstadkoms en liknande effekt på viskositet och ljusspridningsmätningar såväl som kryo-TEM-bilder, där temperaturresponsen kom att likna den för HPMC i rent vatten. 5 vikts-% BDG var tillräckligt för att förändra aggregeringsbeteendet och införa en övergångstemperatur med viskositetsnedgång. Additivets inverkan kan förstås som en effekt av att BDG beter sig som en hydrofob och utrymmeskrävande substituent i MC, i likhet med de stora substituenterna i HPMC och EHEC.

Två instrument, en kvartskristallmikrovåg med dissipation (QCM-D) och en ellipsometer användes för att parallellt bestämma hur ett adsorberat lager av MC och HPMC på kvarts i vatten och i polymerlösning förändras med temperaturen. Kvartsen behövde hydrofobiseras för att adsorption av betydelse skulle kunna ske. Adsorptionen var liknande för båda polymerer vid låga temperaturer. Däremot inträffade en skarp övergång i flera lageregenskaper för HPMC – men inte för MC – nära övergångstemperaturen för viskositeten i bulklösning. Atomkraftmikroskopi (AFM) användes för att mäta attraktiva och repulsiva krafter och även friktionskrafter mellan MC-lager i polymerlösning. Temperaturens påverkan på normalkrafterna var liten, vilket leder till slutsatsen att MC-lagrets yta nästan är helt tömd på hydrofoba grupper. Växelverkan yta–polymer ökar med ökande temperatur och lagret blir mer sammanhängande, vilket leder till större bärförmåga och lägre friktion när mätningen görs vid höga belastningar. AFM användes för att avbilda höjdfördelningen i de adsorberade lagren av MC. Bilderna påvisar att fibrilliknande strukturer bildades vid en lägre temperatur i ytlagret än i bulklösning.

De olika preferenserna för adsorption och aggregering i MC och HPMC ovanför övergångstemperaturerna förklaras av att bildandet av fibriller i MC medför att de hydrofoba delarna hos polymeren avskärmas från lösningen. Därmed motverkas adsorption men även snabb aggregering. Viskositetsnedgången i HPMC och EHEC hänförs till sammandragning inom polymerkedjorna och en aggregering som ger mindre utbredda strukturer.

Table of contents

Preface

Polymers with the property of temperature response have been widely studied during the last decades, and their use is expanding in many fields, including the pharmaceutical, paint and food industries. In opposite to gelatin, some polymers may form gels at high temperatures, whereas they are soluble in water at room temperature.

Cellulose ethers are a group of polymers exhibiting such temperature response. The work presented in this thesis investigates the relation between the molecular structure of different types of cellulose ethers and the effect of temperature on their properties in aqueous solutions and in adsorbed layers. Additionally, the effect of using an amphiphilic liquid as a cosolvent in the cellulose ether solutions is considered.

This thesis presents six articles that have already been published, are submitted for publication or are in close to finalized form. These articles are reprinted in their entirety at the end of the thesis. The subsequent chapters summarize the six articles and the thesis work. The first chapter considers the general background, the second chapter explains the basics of the experimental methods, and the third chapter presents the results.

List of papers

Papers included in the thesis

I. **Aggregation and network formation of aqueous methylcellulose and hydroxypropylmethylcellulose solutions**
Bodvik, R., Dedinaite, A., Karlson, L., Bergström, M., Bäverbäck, P., Skov Pedersen, J., Edwards, K., Karlsson, G., Varga, I., Claesson, P.M.
Published as an article in Colloids and surfaces A 354, 162-171 (2010)

II. **Temperature responsive surface layers of modified cellulose**
Bodvik, R., Thormann, E., Karlson, L., Claesson, P.M.
Published as an article in Physical Chemistry Chemical Physics 13, 4260-4268 (2011)

III. **Temperature-dependent adsorption of cellulose ethers on silica and hydrophobized silica immersed in aqueous polymer solution**
Bodvik, R., Thormann, E., Karlson, L., Claesson, P.M.
Published as an article in RSC Advances 1, 305-314 (2011)

IV. **Temperature-dependent competition between adsorption and aggregation of a cellulose ether – simultaneous use of optical and acoustical techniques for investigating surface properties**
Bodvik, R., Macakova, L., Karlson, L., Thormann, E., Claesson, P.M.
Submitted

V. **Aggregation of modified celluloses in aqueous solution: transition from methylcellulose to hydroxypropylmethylcellulose solution properties induced by a low molecular weight oxyethylene additive**
Bodvik, R., Karlson, L., Thormann, E., Edwards, K., Eriksson, J., Claesson, P.M.
Submitted

VI. **Surface forces and friction between non-polar surfaces coated by temperature-responsive methylcellulose**
Thormann, E., Bodvik, R., Karlson, L., Claesson, P.M.
Manuscript

The author's contribution to the papers

I. Part of planning; most of the experimental work and writing
II. Major part of planning; most of the experimental work; most of the writing
III. Same as paper II
IV. Major part of planning; most of the experimental work; major part of the writing
V. Major part of planning; most of the experimental work; most of the writing
VI. Part of planning; part of experimental work and writing

Summary of included papers

Paper I

In the first paper of this thesis work, we studied aqueous solutions of two types of modified celluloses: methylcellulose (MC) and hydroxypropylmethylcellulose (HPMC). We investigated the temperature related changes in bulk viscosity and molecular association and also the effect of different concentrations of the former. A wide range of techniques were used.

From rheology measurements, light scattering and small-angle X-ray scattering, we found a correlation between viscosity transition and polymer aggregation at high temperatures. The onset temperature for the viscosity changes was affected by polymer concentration and heating rate. The equilibration time was slow, as illustrated by a large difference in viscosity on cooling compared to on heating.

Cryo transmission electron microscopy (Cryo-TEM) was used to image the solutions at different temperatures. It was found that a dense fibrillar network is formed in MC solutions at temperatures above the transition point, marked by a strong viscosity increase. The images of HPMC solutions also showed some formation of fibrillar structures. However, these structures were more linear and less entangled than for MC, explaining the relatively small increase in viscosity in the HPMC solution at high temperature. The characteristic viscosity decrease, which occurs in HPMC solutions at a slightly lower temperature than the viscosity increase, was conferred to the formation of compact structures.

We related the findings to the difference in substitution between the two types of modified celluloses. HPMC has a low degree of hydroxypropyl substituents, which are more bulky than the methoxy groups that are present in both MC and HPMC, preventing close connection between the fibrils formed at high temperatures.

Paper II

In this paper, adsorption of two modified celluloses, a methylcellulose (MC) and a hydroxypropylmethylcellulose (HPMC) was studied. We used three different techniques, quartz crystal microbalance with dissipation monitoring (QCM-D), ellipsometry, and atomic force microscopy (AFM) imaging, to investigate the structure, mass and viscoelastic properties of pre-adsorbed layers at different temperatures. The maximum temperature investigated, 50 °C, was close to the bulk viscosity transition temperature of the MC, but well below that of the HPMC.

Adsorption was conducted at 25 °C, using a very low polymer concentration, followed by a rinsing step with water. The adsorption was insignificant on silica surfaces but clear and for practical purposes irreversible on hydrophobized silica. By following the change in the energy dissipation with adsorption, the adsorption process was found to be typical for polymers forming a single layer. The adsorbing molecules initially attached close to the surface and then formed more extended conformations.

The AFM images and the thickness data from ellipsometry and QCM-D showed that the layers became more compact with increasing temperature up to 50 °C. The effect was reversible, when decreasing the temperature. The compaction after heat treatment, shown by an elasticity increase, was more prominent for the MC. The water content of the adsorbed layers was found to be high at all temperatures studied. This was explained as an effect of water entrapment due to the stiffness of the polymer chains and strong inter-chain contacts. From the AFM imaging it was concluded that the layers are predominately flat with some parts of the polymers protruding into solution. In the case of the MC, the protrusions decreased in height at 45 °C, while for the HPMC no change was seen, which can be explained by its higher transition temperatures in bulk and related to the bulkier substituents.

Paper III

In this paper, the same approach was used, as in the previous one, to study the temperature response up to 50 °C in adsorbed layers of a methylcellulose (MC) and a hydroxypropylmethylcellulose (HPMC) on silica and hydrophobized silica surfaces. Here, however, the layers were immersed in aqueous polymer solution throughout the experiments. QCM-D, ellipsometry, and AFM imaging were again employed to obtain complimentary information on the structure, mass and viscoelastic properties of the polymer layers. It was found that the adsorbed amount increases with increasing temperature, which was explained by the worsening of the solvent quality. The temperature cycling induced a significant adsorption hysteresis. On cooling, desorption of the polymer, previously adsorbed at elevated temperatures, was limited. For each temperature change, the adsorption process needed a long time to reach equilibrium, particularly upon cooling.

The temperature dependence of the adsorption, energy dissipation, layer thickness, water content and viscoelastic properties were found to be similar for the MC and the HPMC, in contrast to what was found for pre-adsorbed layers. It was concluded that the additional adsorption at elevated temperature influenced the layer properties significantly, masking the temperature-response of the initially adsorbed polymer layer. However, AFM imaging showed the same difference between the MC and the HPMC in that the height variations in the layers of the MC decreased considerably when approaching the transition temperature, while no change was observed in HPMC layers.

Paper IV

This paper was a continuation of the study of hydroxypropylmethylcellulose (HPMC) adsorption from an aqueous solution onto hydrophobized silica. We made use of new equipment, which allowed us to run ellipsometry and QCM-D measurements simultaneously to probe the same substrate immersed in polymer solution. It also gave us the possibility to follow the layer properties up to 80 °C, which was well above the bulk viscosity transition temperatures of the studied HPMC.

Below the bulk transition temperatures, the adsorbed amount was slowly increasing with temperature. Around the bulk transition temperatures and higher, the increase in adsorbed mass and the changes in layer properties were dramatic. Several layer properties such as adsorbed mass, sensed mass, layer thickness, water content and viscoelasticity all showed a transition temperature on heating that closely coincided with the bulk transition temperatures. The interfacial transition temperatures were correlated to the polymer aggregation and viscosity changes that we had observed in light scattering and rheological measurements. We related this clear correlation to a newly proposed model that considers competition between aggregation and adsorption/deposition. This model predicts that surface-induced instability (deposition on the surface) should occur just before bulk instability (aggregation in the solution).

Comparing our results on methylcellulose (MC) and HPMC layers and another study on ethyl(hydroxyethyl)cellulose (EHEC) layers above the respective transition points, we found that the temperature response was much larger in adsorbed layers of HPMC and EHEC than in layers of MC. Thus, in the case of MC, bulk aggregation appeared to be favoured over deposition, in opposite to what the aforementioned model predicted. We explained this by the possibility in the MC layers for a more significant depletion of hydrophobic regions from the layer–solution interface compared to in the HPMC or EHEC layers. Hydrophobic interaction is the mechanism we propose as responsible for bulk aggregation as well as for additional adsorption at high temperatures.

Paper V

In the fifth paper we returned to bulk studies, investigating the temperature effects on viscosity and aggregation behaviour of aqueous solutions of three different cellulose ethers. The same methylcellulose (MC) and hydroxypropylmethylcellulose (HPMC) were used as in papers II-IV and for comparison an ethyl(hydroxyethyl)cellulose (EHEC) was also investigated. Like in paper I, the techniques employed were viscosity and dynamic light scattering measurements and Cryo-TEM. The association behaviour of methylcellulose was also investigated in mixtures of water and the amphiphilic liquid diethyleneglycolmonobutylether (BDG).

An increase in temperature reduces the solvent quality of water for all three polymers, inducing an increase in aggregate sizes as observed using light scattering. It was found that the aggregation rate followed the order EHEC > HPMC > MC, suggesting that cellulose ethers containing some bulky and partly hydrophilic substituents assemble into large aggregates more readily than methylcellulose. The bulkiness hinders the formation of fibrils, which are characteristic for MC from temperatures around the transition temperature and higher. The fibrils in turn counteract the kinetics of the self-assembly into large aggregates, since the hydrophobic parts of the chain are shielded efficiently in the fibrillar structure, which explains the order of aggregation rates for the different cellulose ethers.

When the concentration of BDG was at and above 5 wt%, methylcellulose adopted a solution behaviour that is typical for HPMC and EHEC, exhibiting two transition points: one temperature, where the viscosity decreases; and another, slightly higher, temperature, where it increases. The aggregation rate also increased on adding BDG to resemble the HPMC behaviour in water. In the water/BDG 90:10 mixture, MC no longer formed fibrils at elevated temperatures. We concluded that BDG, due to its ability to accumulate at non-polar interfaces may act as a physisorbed hydrophilic and bulky substituent in the abundantly hydrophobic MC chain. Thus, it induces similar constraints on aggregation as the chemically attached hydroxypropyl groups in HPMC and oligo(ethyleneoxide) chains in EHEC.

The onset temperature for aggregation occurred at a temperature similar to, or lower, than the viscosity transition temperatures. Thus, the decrease in viscosity could not be correlated to the onset of aggregation, but is likely due to intra-chain contraction and aggregation into less extended structures.

Paper VI

In this paper we used the AFM colloidal probe technique to investigate temperature effects from 25 °C to 50 °C on surface forces and friction between adsorbed layers of methylcellulose (MC) on hydrophobized silica surfaces in contact with an aqueous MC solution.

We also employed AFM in PeakForce tapping mode to obtain images at the same temperatures, illustrating the changes in height and deformation in the surface layer. At the lowest temperature the conformation was rather flat with some protruding polymers or aggregates, which became more abundant at higher temperatures. We found evidence for formation of fibril-like aggregates within the adsorbed layer already at 40 °C, which is significantly lower than the aggregation onset temperature in the MC bulk solution. The structures were similar to those we had previously found using Cryo-TEM and described in Papers I and V. We explained the lower aggregation temperature in the adsorbed layer by the smaller entropy decrease, compared to the case in bulk solution, since a large portion of the conformational entropy is lost during adsorption.

It was found that the normal surface forces are rather insensitive to temperature. We conferred this to accumulation of the hydrophobic groups within the layer, and further shielding of these groups by formation of fibrillar structures at higher temperatures. No strong attractive forces were observed, which was expected, since the temperatures studied were lower than the bulk transition temperature.

In contrast, the friction forces changed significantly with increasing temperature. At low loads the friction increased with increasing temperature as a result of increasing attraction between segments within the surface layer, not due to bridging forces between the layers. At high loads the reverse was observed, the friction decreased with increasing temperature. This is a consequence of higher load bearing capacity of the MC layer induced by the worsening of the solvent quality resulting in stronger polymer–surface affinity and better cohesion within the layer.

1. Background

a. Temperature responsive polymers

Polymer films can be used to control the release of active substances, utilizing a range of different stimuli as for example temperature, light, salt concentration and pH.[1] Depending on the choice of polymer, delivery of a substance can for instance be made to incease at high or low temperatures.[2] The development of temperature responsive polymers and their use in surface layers is of great interest for the food,[3] mineral processing,[4] coating [5] and pharmaceutical industries.[6] To this end polymer structures containing *e.g.* poly(*N*-isopropylacrylamide) (PNIPAAm),[7-11] poly(2-isopropyl-2-oxazoline),[12] poly(2-(dimethylamino)ethyl methacrylate,[13] poly(ethylene oxide)(PEO) [14-15] and poly(propylene oxide) [16] chains, exhibiting negative temperature response, can be utilized. Such polymers are water soluble at lower temperatures, but phase separate above their respective lower critical solution temperature (*LCST*). In this thesis work the temperature response of cellulose ethers is of particular interest.

i. Cellulose ethers

Cellulose ethers are an important class of temperature responsive polymers.[17] While unmodified cellulose is insoluble in water, modification of the cellulose chain by attachment of small substituents, as shown in Figure 1, may result in water solubility and temperature responsive properties. Cellulose ethers exhibit negative temperature response as they undergo a transition above a certain temperature, where the viscosity of their aqueous solutions increases due to worsening of the solvent quality. In some cases the transition leads to gel formation; this is a common feature of methylcellulose (MC). The gel properties are governed by the exact type of substitution.[18-19] Hydroxypropylmethylcellulose (HPMC) and ethyl(hydroxyethyl)cellulose (EHEC) are two cellulose ethers with a certain degree of substituents with hydroxyl end groups. These two polymers exhibit a decrease in viscosity at a temperature slightly below the one where the viscosity increases. In each case the transition temperature depends on the degree of substitution. To emphasize this aspect: the methylcelluloses will be referred to as M_xC; the hydroxypropylmethylcelluloses as HP_yM_xC; the ethyl(hydroxyethyl)celluloses as E_zHE_qC; where x is the methoxy degree of substitution, y the hydroxypropyl molar substitution, z the ethoxy degree of substitution and q the hydroxyethyl molar substitution. The typical viscosity temperature responses of MC and HPMC are shown in Figure 2. The lower critical solution temperature of MC and HPMC is between 40 and 50 °C and between 75 and 90 °C, respectively.[20-21]

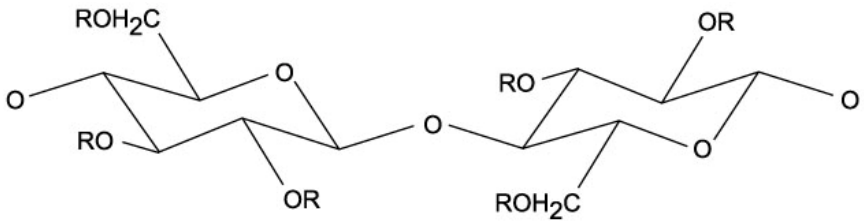

Figure 1. Structure of modified cellulose: in methylcellulose R = H or CH_3; in hydroxypropylmethylcellulose R = H, CH_3 or $CH_2CH(OR')CH_3$; in ethyl(hydroxyethyl)cellulose R = H, CH_2CH_3 or CH_2CH_2OR'; R' represents a new R group.

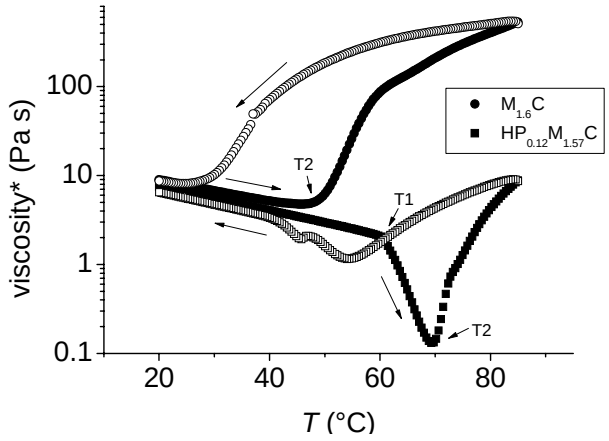

Figure 2. Change in complex viscosity for an MC and an HPMC, referred to as $M_{1.6}C$, $HP_{0.12}M_{1.57}C$ respectively, where the numbers after M are the methoxy degrees of substitution and the number after HP is the hydroxypropyl molar substitution, on increasing (filled symbols) and decreasing (open symbols) the temperature. The direction of the temperature sweep is indicated by arrows.

Cellulose ethers find use in many applications, *e.g.* as thickeners, water binders, film forming agents and in controlled release, due to the fact that their temperature response can be modified by small changes in the degrees of substitution.[17, 22-23] They have been used in the fields of biotechnology,[24] paints,[25] pharmaceuticals [26-27] and foods.[28] Several cellulose ethers share the same temperature responsive behaviour. Besides methylcellulose (MC) [29-31] and hydroxypropylmethylcellulose (HPMC),[32] ethyl(hydroxyethyl)cellulose (EHEC) [33-52] is a very well-studied example. MC has been used to enhance drug release from microcrystals, [29] and functionalized by laminin it has been utilized in neural tissue engineering.[53-54] HPMC may form chelate complexes with Ca^{2+}, which improves its use in injectable biomaterials for bone and dental surgery.[53] HPMC in combination with ethylcellulose has also been used as a coating on drug-loaded silica gels to control the drug release profile.[54] In this application it was found that the HPMC undercoating suppressed the drug release by making the core surface softer and facilitating formation of a continuous ethylcellulose film.

ii. Methylcellulose (MC)

It was noted by Sarkar that the transition temperature showed a very limited molecular weight dependence for commercial MC samples, which could be explained by the high polydispersity and the high molecular weight fraction present also in samples with low average M_w.[55] MC can be prepared by two different routes, one giving a uniform and the other a random distribution of substituents along the chains.[56-57] The uniformly substituted MC does not gelate at the degrees of substitution needed for providing water solubility. Therefore, only the heterogeneous type, which is water soluble when the degree of substitution is between 1.3 and 2.6, is used commercially.[57] Extensive aggregation occurs only when the degree of substitution is larger than 1.2-1.5.[58-59] The water solubility of modified cellulose polymers is primarily attributed to the reduced number of inter-chain hydrogen bonds.[60] However, if the degree of substitution of MC is too high, the hydrophobicity of the methoxy groups renders the polymer insoluble in water.[56] A change in hydration with temperature has been indicated by calorimetry measurements, where an endothermic peak is observed upon heating and an exothermal peak upon cooling.[61-65] Water molecules are prone to form a cage-like structure around small non-polar solutes,[66-67] and it has been suggested that water arranges similarly around the hydrophobic substituents on modified cellulose polymers.[60-61]

This type of hydration is enthalpically favourable but entropically unfavourable.[68] As the temperature increases the entropy term becomes more important and the free energy of the system is reduced by aggregation, in analogy to formation of micelles from surfactant monomers. Thus, the aggregation and gelation process is entropy driven.[69] For HPMC hydrogels it has also been found by calorimetry[70-71] that a significant fraction of water does not freeze until the temperature is well below 0°C, which is due to polymer-water interactions. This has been confirmed by dielectric spectroscopy measurements that report several melting transitions at sub-zero temperatures.[72]

The slow aggregation at lower temperatures, as well as the gelation and phase separation of MC at the *LCST*,[73] has been attributed to hydrophobic association.[57] According to Kato et al.,[62] the first stage reflects the association of the most hydrophobic trisubstituted glucose units, while gelation occurs when also di- and monosubstituted units aggregate. The presence of trisubstituted glucose units has later, by Nakagawa et al., been shown to be essential for gel formation.[18] It has been suggested that also free hydroxyl groups on the less substituted glucose units contribute to the association process by forming inter-chain hydrogen bonds.[74-75] The gel is not homogeneous, but contains microphase-separated regions as evidenced from NMR and SANS measurements.[20, 56, 76-78] Joshi et al. distinguish between a hydrophobic association step and a following swelling upon further heating.[79] As the temperature of an aqueous MC solution is increased, the dynamic storage modulus increases slowly up to the gelation temperature, where a sharp increase and a high plateau value is obtained.[55, 62, 80] A decrease in temperature leads to disaggregation, and a subsequent large decrease in storage modulus. However, this transition occurs at a temperature far below the gelation temperature,[60] demonstrating the importance of kinetically trapped non-equilibrium states.

iii. The effect of hydroxyalkyl substituents

The presence of hydroxypropyl substituents, in addition to methyl substituents, results in a more complex solution behaviour.[55, 81] When an HPMC solution is heated the storage modulus first decreases, at a temperature denoted $T1$, followed by an increase at higher temperature, referred to as $T2$.[81-82] It has been proposed that the cloud point and phase separation may occur at the point of modulus decrease[83] rather than at the point of modulus increase, as reported for MC.[56] Another difference between MC and HPMC is that the substituents in MC become largely immobile at high temperatures, whereas they remain solvated in HPMC and also in the non-gelling hydroxypropylcellulose.[20, 84-85] NMR data indicates that hydroxypropyl modification inhibits inter-molecular association.[86] A remarkable feature is that addition of only small quantities of hydroxypropyl substituents to MC changes the solution and rheological behaviour significantly.[55]

b. Additives

Various types of low molecular weight additives are often used in order to modify the properties of polymer solutions. For instance, addition of different salts affects the transition temperatures of PNIPAAm and other polymers in accordance with the Hofmeister series. This does not necessarily change the transition qualitatively, in terms of viscosity, phase separation or clouding, even though complete transition may take place over a broader temperature range and in more steps compared to when no salt is added.[87] In order to reduce the viscosity of polymer solutions other types of additives may be used like alcohols or surfactants.

i. Glycol ethers

Glycol ethers are low molecular weight liquids with very good, in many cases complete, miscibility with

water. They may consist of 1-3 oxyethylene units and an aliphatic chain, with 1-6 carbon atoms.[88] The amphiphilic structure of glycol ethers with one lipophilic and one hydrophilic part, illustrated in Figure 3, gives them surfactant-like properties in water mixtures, where they decrease the surface tension [89] and enhance the wetting of non-polar substrates.[88] Glycol ethers are good solvents for cellulose ethers. Two glycol ethers, diethyleneglycolmonobutylether (also called butyldiglycol and abbreviated BDG; structure shown in Figure 3) and triethyleneglycolmonobutylether (butyltriglycol, BTG) are commonly used for cellulose ether preparation in paint applications. They are known to counteract the association between hydrophobically modified cellulose ethers in aqueous solutions, where they act as less polar solvents compared to water.[25] Previously, EHEC has been studied in water/BDG mixtures, comparing the effect of the additive using unmodified or hydrophobically modified EHEC samples with different side chain lengths and densities.[36, 90] In this thesis work we explored the effect of BDG on the aggregation properties of MC solutions, and compared the behavior to that of HPMC and EHEC aqueous solutions in the absence of BDG.

Figure 3. The structure of diethyleneglycolmonobutylether, BDG, consisting of 2 oxyethylene units linked to a butyl chain.

ii. Comparison of BDG to other polymer solution additives

Courtenay et al. propose that the effect of protein denaturants such as urea and guanidinium salts is similar to the effect of anions and cations in the Hofmeister series and also of neutral cosolutes. This was attributed to a change in the water accessible surface area on the solute induced by the additive.[91]

On one end of the Hofmeister series are the chaotropic anions. They have a salting-in effect that leads to a higher solubility for nonpolar solutes. In PNIPAAm aqueous solutions the chaotropic effect has been attributed to direct binding of the additive to the polymer or to a surface tension mechanism.[87] The surface tension typically decreases on addition of chaotropic ions. The transition temperature may increase or decrease slightly using these additives. Urea and BDG presumably acts in a similar way. They also induce a lower surface tension, which is accompanied by a small decrease or increase in transition temperature. In contrast to chaotropic anions, the kosmotropic anions are strongly hydrated. Due to this hydration, the dissolution mechanism of kosmotropes for PNIPAAm aqueous solutions is based on the polarization of the ions. In this type of solution they induce a large decrease in transition temperature.[87]

c. Polymer adsorption

Adsorption of uncharged polymers, as considered in this thesis work, is in general a complex process, and depends on a range of factors. For a detailed description the reader is referred to the excellent book by Fleer et al.[92] The structure of the polymer, *e.g.* if the chain is linear or branched, the molecular weight, the stiffness of the polymer chain, the sequence of the polymer segments (homopolymer, random co-polymer or block co-

polymer) all influences adsorption. The cellulose ethers used in this thesis work can be seen as relatively stiff (persistence length ≈ 60 Å) linear and polydisperse random co-polymers where the different segments have different degrees of substitution.

Adsorption is also affected by the polymer–solvent interaction, as expressed by the chi-parameter. In general one expects an increased adsorption as the solvent quality, *i.e.* the polymer affinity for the solvent, is reduced. A change in solvent quality may also affect the polymer–surface affinity, and in general an increase in the surface–polymer interaction parameter results in higher adsorbed amount. In this thesis work we have utilized temperature changes to influence the solvent quality of water for MC and HPMC. Some previous work that has utilized the same stimuli to tune polymer adsorption is recapitulated below.

i. Temperature responsive polymers

The effect of temperature on adsorption and layer structure has been investigated for some temperature responsive polymers, including poly(*N*-isopropylacrylamide) and EHEC, using techniques such as quartz crystal microbalance[7, 93-96], ellipsometry [35, 41] and surface force techniques.[7, 16, 33, 39-40, 42] The conformation of EHEC on hydrophobized mica was in earlier studies shown to be relatively flat, and the main driving force for the adsorption was suggested to be hydrophobic interactions.[39] The adsorbed amount increased upon temperature increase, and then decreased as the temperature subsequently was decreased again.[41] The forces between two such EHEC-coated surfaces stayed repulsive but became less long-ranged upon heating to several degrees above the cloud point, suggesting that the most hydrophilic segments were oriented towards the solution.[40] Higher above the cloud point, an attractive force was observed.

In another study HPMC was found to form very elastic films at the air-water interface, even at low surface pressures.[23, 97] High coverage of the interface was reached at very low concentrations in the bulk phase. With increasing bulk concentration the monolayer structure finally collapsed. Differences in surface activity between different HPMC samples were attributed to different hydroxypropyl molar substitution and molecular weight. Similar viscoelasticity and elastic dilatational modulus for the investigated samples was explained by a similar degree of methyl substitution.

2. Description of techniques

a. Light Scattering

Scattering is one of several ways that light may interact with a sample. It is different from transmission, where light passes the sample without interaction, and adsorption, where the photons lose part or all of their energy and hence change frequency. Scattering is caused by the electric field in the light beam making the electrons contained within the atoms of the sample start to oscillate around their equilibrium positions. Radiation is emitted from the sample due to the change in charge velocity. The scattered light leaves the sample in a plane perpendicular to the oscillation.

If the energy (and frequency) difference between the incident beam and the scattered light is negligible, the sample is called a Rayleigh scatterer and the scattering elastic. Intensity or static light scattering are other names for the same phenomenon.

There are two main factors that give rise to changes in frequency: particle motion and changes in the internal energy states of the molecules in the sample. The effect of particle motion is similar to the Doppler shift for sound waves. It is related to the size of the molecules, which may be determined using dynamic light scattering, a technique that has also been called photon correlation spectroscopy or quasi-elastic light scattering. A change in the internal energy states in the sample molecules is related to the photons either losing or gaining energy through interaction with the sample. In dynamic light scattering, by the use of an autocorrelator, one measures intensity fluctuations caused by molecular motions.

i. Static light scattering (SLS)

First, we will consider the scattering by a single gas atom in vacuum. Light consists of an electric and a magnetic field that are perpendicular to each other. In the following, we will only consider the electric field, which for plane polarized and monochromatic light propagating in the *x*-direction is given by:

$$E = E_0 cos\left[2\pi(\nu t - \frac{x}{\lambda})\right] \quad (1)$$

where E is the electric field strength, ν the frequency, x the length of propagation, and λ the wavelength. E_0^2, *i.e.* the square of the wave amplitude is proportional to the intensity, defined as the rate of flow of radiation per area unit.

The oscillating dipole created, when the atom is hit by the incident light, has a dipole moment $\mu=\alpha E$, where α is the polarizability of the atom. The resulting electric field is caused by the acceleration of electrons and the field strength of the scattered light is proportional to the second derivative of the dipole moment with respect to time. The intensity of light scattered from a single particle normalized by the incident light intensity and geometrical factors can be expressed by the Rayleigh ratio, R_Θ:

$$R_\Theta = 16\pi^4\alpha^2/\lambda^4 \quad (2)$$

The polarizability is also proportional to the particle volume, from which follows that the scattered intensity is proportional to the sixth power of the particle radius.

The theory can be extended from the case of a single atom to a dilute polymer solution using the following expression for the scattering intensity:

$$I(q) = KMcP(q)S(q) = \left(\frac{4\pi^2 {n_0}^2 (\mathrm{d}n/\mathrm{d}c)^2}{N_\mathrm{A}{\lambda_0}^4}\right) McP(q)S(q) \quad (3)$$

where n_0 is the refractive index of the solvent, dn/dc the refractive index increment, λ_0 the wavelength of the laser beam in vacuum, N_A the Avogadro number, M the weight-averaged mass of the polymer, and c the polymer mass concentration. The parameter q is the modulus of the scattering vector and q=4π$n_0$sin(θ)/λ, where 2θ is the angle between incident and scattered beam and λ is the wavelength of the light. $P(q)$ is the polymer normalized form factor ($P(q$=0)=1). The structure factor $S(q)$, which for very dilute solutions is $S(q)$=1, describes concentration effects. Thus, if aggregation occurs without change in the scattering contrast (dn/dc), then the scattered intensity at small q-values will increase due to the increase in M. The radius of gyration, R_g, can be derived from an expression for $P(q)$.

ii. Dynamic Light Scattering (DLS)

Particles in solution are always under the influence of so called Brownian motion, which is related to the diffusion of the particles due to the interplay of osmotic and viscous forces. When the particles move in parallel or in opposite direction to incident radiation, the observed frequency of the scattered light respectively increases and decreases. The speed distribution of the particle motion gives rise to a line-width broadening of the scattered light signal.

The autocorrelator monitors the concentration fluctuations by repeatedly multiplying the intensity during a short time interval (in the order of 1 μs) at time t by the intensity at time t+Δt. The calculation is repeated at least 10^5 times for all intensity products within the chosen time limits. The measured values are described by the intensity (or second-order, denoted with a subscript) autocorrelation function $G_2(t)$= $I(t)I(t$+Δ$t)$, where $I(t)$ is the intensity at delay time t. The averaged intensity products are the highest at short delay times and decrease when the monitored intervals become more separated. When the intervals are close in time the two measured intensities will be similar, since the molecules do not have time to collide between the measurements. This means that the product ‹$I(t)I(t$+Δ$t)$› will be close to ‹I^2›. At long delay times it will approach ‹I›^{2}, as the intensities become less and less correlated.

The physical quantities of interest are related to the electric field (or first-order, denoted with a subscript) autocorrelation function, $g_1(t)$, which is obtained from the second-order function using the Siegert relationship:

$$G_2(t) = Bg_2(t) = B(1 + \beta^2|g_1(t)|^2) \quad (4)$$

where B=‹I›^{2} is the baseline value at infinite delay time and β is a parameter accounting for the coherence of the laser beam and detector optics. Lowercase g denotes the autocorrelation function normalized by dividing with B.

In the case of monodisperse samples the decay can be described by a single-exponential function:

$$|g_1(t)| = e^{-\Gamma t} \quad (5)$$

where Γ is the decay or relaxation rate, which for dilute systems is:

$$\Gamma = D_\mathrm{T} q^2 \quad (6)$$

where D_Γ is the translational diffusion coefficient and q the modulus of the scattering vector, defined by:

$$q = \frac{4\pi n_0 \sin(\theta)}{\lambda} \quad (7)$$

where 2θ is the angle between incident and scattered beam and λ is the wavelength of the light.

In dilute solutions, the translational diffusion approaches a value D_0, from which particle size can be obtained using the Stokes-Einstein formula:

$$D_0 = \frac{kT}{3\pi\eta_0 d_\mathrm{h}} \tag{8}$$

where k is the Boltzmann constant, T the temperature, η_0 the solvent viscosity and d_h the hydrodynamic diameter of the particle.

A traditional way of obtaining the decay rate and subsequently structural data is by fitting the data to a cumulant expansion of the logarithmized single-exponential function. The autocorrelation function $g_1(t)$ is in the cumulant expansion given by:

$$\ln\left(g_1(t)\right) = -\Gamma t + \frac{\mu_2}{2}t^2 - \frac{\mu_3}{3}t^3 + \cdots \tag{9}$$

where Γ, μ_2 and μ_3 are the first, second and third cumulants. For polydisperse systems, the first cumulant represents the z-average of the decay rate, giving the translational diffusion coefficient, in accordance with Equation 6.[98] The polydispersity index, *PDI*, is defined by the relation:[99]

$$PDI = \frac{\mu_2}{\Gamma^2} \tag{10}$$

which is a measure of the width of the decay rate distribution.

For polydisperse samples, a more complicated analysis may be needed. In the simplest case of polydispersity the electric field autocorrelation function is a sum of two exponential functions. Generally it is an inverse Laplace transform of the distribution of decay rates. Several methods have been developed for performing the inversion of the transform in order to obtain the decay rate distribution, which in turn gives the size distribution in the polydisperse sample. Two examples are the CONTIN and NNLS (Non-Negatively Restricted Least-Squares) methods.

b. Rheology

In this thesis work the complex viscosity of different bulk solutions were obtained from oscillation strain control measurements. A sample was put under a constant strain while applying an oscillating stress. A temperature sweep was carried out starting at 10 °C, heating to 85-90 °C, and then cooling to 10 °C again. Heating/cooling rates between 0.1-1.5 °C/minute were used. The temperature control was assured by Peltier concentric cylinders, which allows a maximum heating rate of 13 °C/min. Four heating elements are placed in contact with the lower cup geometry, providing efficient heat transfer up the walls of the cup. The elements are held in place by an insulated jacket. A platinum resistance thermocouple is placed close to the top of the cup ensuring accurate temperature measurement and control.

c. Cryo Transmission Electron Microscopy (Cryo-TEM)

Cryo Transmission Electron Microscopy (Cryo-TEM) is a technique for imaging structures that have been preserved in a certain state by freezing a thin film obtained from a bulk solution. An electron beam is transmitted through the sample, giving an image, which can be magnified to a resolution of 4-5 nm. The sample needs to be thinner than 500 nm, due to the amount of scattering of electrons within the sample and also to allow rapid freezing of the film. When preparing a sample, the solution to be imaged is first set to the conditions, *i.e.* humidity and temperature, of interest.

A small drop from the sample solution is then placed on a microscopy grid, which is covered by a perforated polymer film, and blotted with a filter paper to obtain a thin sample layer covering the holes in the film. By rapid plunging into a cooling liquid, like ethane near the freezing point, the sample is vitrified. The vitrified sample is transferred to the TEM, where it is examined while cooled with liquid nitrogen.

d. Quartz Crystal Microbalance with Dissipation (QCM-D)

Quartz Crystal Microbalance (QCM) measures frequency changes in a quartz crystal due to adsorption. When also measuring the energy dissipation the instrument is called QCM-D. In addition to mass changes and adsorption kinetics it then also provides information on film viscosity and elasticity.[100]

The main parameter determined using QCM-D is the sensed mass. For rigid layers it can be calculated from the Sauerbrey relation, which states that the change in the oscillation frequency is linearly related to the mass added to the crystal, including water associated with the adsorbed layer.[101] However, the Sauerbrey relation does not hold for viscoelastic layers.[102] This situation should be indicated by a difference in the Sauerbrey mass calculated from the different overtones, and in such a case a viscoelastic model is normally needed.[103] The Voigt model is one such viscoelastic model. It consists of two elements, connected in parallel: a viscous damper, where the stress is directly proportional to the rate of strain, and an elastic spring, where the stress is directly proportional to the strain.[104] While the shear strain is the same for both elements of the model, the total shear stress is the sum of both contributions:

$$\sigma_{xy} = \mu_{\mathrm{f}} \frac{\partial u_x(y,t)}{\partial y} + \eta_{\mathrm{f}} \frac{\partial v_x(y,t)}{\partial y} \tag{11}$$

where the first term is the elastic part (from Hooke's law) and the second term the viscous part (from Newton's law of viscosity). μ_{f} denotes the shear elastic modulus, and η_{f} the shear viscosity, of the film. u_x is the displacement, and v_x the velocity in the x-direction. The (x,y)-plane is defined to be parallel to the crystal.

The viscoelastic properties of the film are related to the changes in frequency and dissipation through the β parameter,[103-104] which is obtained by solving the wave equation for bulk shear waves propagating in the medium:

$$\Delta F = \mathrm{Im}\left(\frac{\beta}{2\pi t_{\mathrm{q}} \rho_{\mathrm{q}}}\right) \tag{12}$$

$$\Delta D = -\mathrm{Re}\left(\frac{\beta}{\pi F t_{\mathrm{q}} \rho_{\mathrm{q}}}\right) \tag{13}$$

where F is the frequency, t_{q} is the thickness, and ρ_{q} the density, of the quartz oscillator.

If needed, the Voigt model can be extended, taking into account the frequency dependence of the viscosity and/or elasticity.[105] In this work the extended model was used in the analysis.

e. Ellipsometry

Ellipsometry is a technique that utilizes the change in polarization upon reflection of plane polarized light. Two optical parameters, the refractive index and the thickness, of a film (modelled as one or several layers) adsorbed on a well-defined substrate can be determined from changes in the positioning of the instrument components. The adsorbed amount in the film is calculated from these two parameters and can be followed over time in solution or measured directly in air.

In this thesis work the null ellipsometry method was utilized. The instrument components, which are configured in the order Polarizer-Compensator-Substrate-Analyzer are in this method set to minimize the effect of the refracted beam (*i.e.* make the beam linearly polarized). A thorough description of the instrumental set up has been published elsewhere.[106]

The measured parameters are the ellipsometric angles Ψ and Δ, which are measured continuously and used to calculate the mean thickness (d_f) and refractive index (n_f) of the adsorbed layer.[107] While both the thickness and refractive index are very sensitive to small changes in the ellipsometer angles, the variations in these parameters are coupled.[108] This explains why the adsorbed mass, which is proportional to the thickness and the difference in refractive index between the layer and the bulk, is obtained with a better accuracy than either of these two parameters.

The adsorbed mass, Γ, was in this work calculated using the de Feijter formula:[109]

$$\Gamma = d_f \frac{n_f - n_{buffer}}{dn/dc} \quad (14)$$

where dn/dc is the polymer refractive index increment, which can be determined using a refractometer, d_f the film thickness, n_f is the refractive index of the film and n_{buffer} the refractive index of the buffer.

f. Analysis of adsorption data

The combination of results from acoustical and optical techniques for adsorption study provide some useful information. An effective hydrodynamic thickness, d_{eff}, of the adsorbed layer may be calculated from the following expression:[105, 110]

$$d_{eff} = \frac{m_{sensed}}{\rho_{eff}} = \frac{m_{sensed}}{\rho_{pol}\left(\frac{\Gamma}{m_{sensed}}\right) + \rho_{sol}\left(1 - \frac{\Gamma}{m_{sensed}}\right)} \quad (15)$$

where m_{sensed}, obtained from an acoustical technique, is the sensed mass, which includes water associated with the adsorbed layer, ρ_{eff} the effective density of the layer, Γ the polymer adsorbed amount, obtained from an optical technique, ρ_{pol} the polymer density and ρ_{sol} the density of the solvent.[111]

Since the adsorbed mass obtained by the optical technique is due to the adsorbing species only, the water content of the layer can be calculated from:

$$\%water = \frac{m_{sensed} - \Gamma}{m_{sensed}} \times 100 \quad (16)$$

g. Simultaneous use of optical and acoustical techniques

The effect of temperature on adsorption and structure of surface layers can be investigated using a range of different techniques.[112] Previously, adsorption of PNIPAAM and EHEC has been studied using optical, acoustical and surface force techniques.[35, 94, 113]

The interest in utilizing acoustical or electroacoustical techniques for the monitoring of thin films has increased during the past decades. One example of such a technique is the quartz crystal microbalance (QCM), briefly described above. The mass change determined by QCM includes the mass of the adsorbing species as well as the mass of hydrodynamically trapped solvent.

For the study of adsorbed species only, not taking into account solvent present in the films, optical techniques are commonly used. Examples of this are surface plasmon resonance (SPR), ellipsometry, reflectometry, reflectometric interferometric spectroscopy and optical waveguide techniques, which all measure two key parameters: thickness and refractive index.[114] From these data the adsorbed amount can be calculated.

Information on the solvent content or porosity of a thin film is most conveniently obtained by combining acoustical and optical techniques.[115] Such studies may be performed using similar substrates in the different techniques, but an approach that uses two techniques to simultaneously study exactly the same substrate has clear advantages. For instance, errors due to variations in the substrate and experimental conditions like mass transport parameters can be disregarded. Earlier examples of simultaneous acoustical and optical probing of the same support include QCM with grating assisted SPR [116] or ellipsometry.[117] Recently, equipment has been developed for the simultaneous use of QCM-D with optical reflectometry,[114] or with spectroscopic ellipsometry.[118-120] A few different systems have been studied by optical and acoustical techniques in tandem include organic surfactants, self-assembled monolayers, multiple-layer target DNA,[121] and polymer brushes.[117] In this thesis work we used QCM and ellipsometry to simultaneously investigate adsorption of cellulose ethers as a function of temperature.

3. Results and discussion

a. Modified celluloses

The cellulose ethers that were investigated in this thesis work are recapitulated in Tables 1 and 2. In this section we will use the designations, highlighting the degree of substitution and molar substitution, previously used in Papers II-VI.

Table 1. Substitution and viscosities of cellulose ethers from Dow, used in Paper I.[111]

Sample	Trade name	Viscosity† (Pa·s)	Methoxy degree of substitution	Hydroxy-propyl molar substitution	M_w (kDa)
$M_{1.8}C$	A16M	16	1.8	-	160[a]
$HP_{0.13}M_{1.8}C$	F4M	4	1.8	0.13	70[a]
$HP_{0.21}M_{1.4}C$	K15M	15	1.4	0.21	ca. 160[b]

† of 2 wt% aqueous solutions at 20 °C

[a] Based on light scattering measurements reported in Paper I

[b] Estimation based on the viscosity

Table 2. Substitution and viscosities of cellulose ethers from Akzo Nobel, used in Papers II-VI.

Sample	Viscosity† (Pa·s)	Methoxy degree of substitution	Hydroxy-propyl molar substitution	Ethoxy degree of substitution	Hydroxy-ethyl molar substitution	M_w (kDa)
$M_{1.6}C$	20	1.6	-	-	-	530
$HP_{0.12}M_{1.57}C$	20	1.57	0.12	-	-	620
$E_{1.3}HE_{1.5}C$	4	-	-	1.3	1.5	ca. 300[a]

† of 2 wt% aqueous solutions at 20 °C

[a] Estimation based on the viscosity

b. Bulk properties

i. Viscosity

In our rheology measurements the main parameter obtained was the complex viscosity μ^*, which is defined as $\mu^* = \sqrt{G'^2 + G''^2} \,/\, 2\pi f$, where G' and G'' are the storage and the loss moduli respectively, and f is the frequency.[36] The typical rheological temperature response of methylcellulose in aqueous solution is shown in Figure 1, where the complex viscosity of three different $M_{1.8}C$ solutions is shown as a function of temperature for different polymer concentrations. The bulk transition occurs at a temperature $T2$ and the viscosity increases dramatically, particularly

when the MC gelates, which is the case for this MC with a methoxy degree of substitution of 1.8. From room temperature up to *T*2 the viscosity change is correlated to the change in water viscosity, which is illustrated by the lower curve in Figure 1. The *T*2 temperature of the MC may have significant concentration dependence as shown in Figure 2a. It should be noted that this illustrates the bulk concentrations needed for large viscosity changes. Other bulk changes, like aggregation, may occur at very low concentrations and without large deviations from the *T*2 temperature. This will be further discussed below. The slow kinetics of the molecular rearrangements in the MC solution is clear from the large hysteresis on cooling, where the viscosity is kept at high values until temperatures well below *T*2 are reached. The importance of non-equilibrium states is also shown by the significant dependence of the *T*2 value on the sweep rate (see Figure 2b). A practical estimation of *T*2 can be made by linear extrapolation of the data to zero sweep rate. The value thus obtained for a 1 wt% solution of $M_{1.8}C$ is *T*2 = 42 °C and for a 0.75 wt% solution of $M_{1.6}C$ *T*2 = 51 °C.

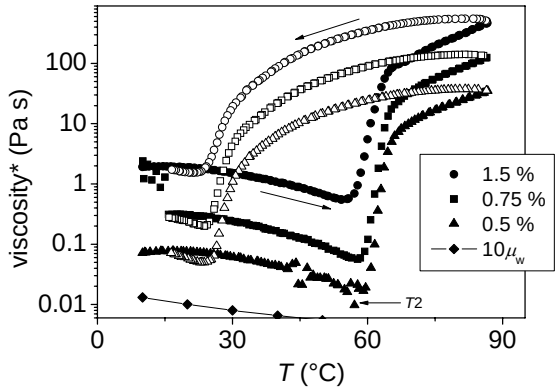

Figure 1. Complex viscosity as a function of temperature (sweep rate 1.5 °C /min) for $M_{1.8}C$ solutions of different concentrations. Filled and unfilled symbols correspond to data obtained on heating and cooling, respectively. Arrows along the curve indicate the direction of the temperature sweep. The *T*2 temperature is also shown. The lower curve represents the viscosity of water, multiplied by ten, as a function of temperature.

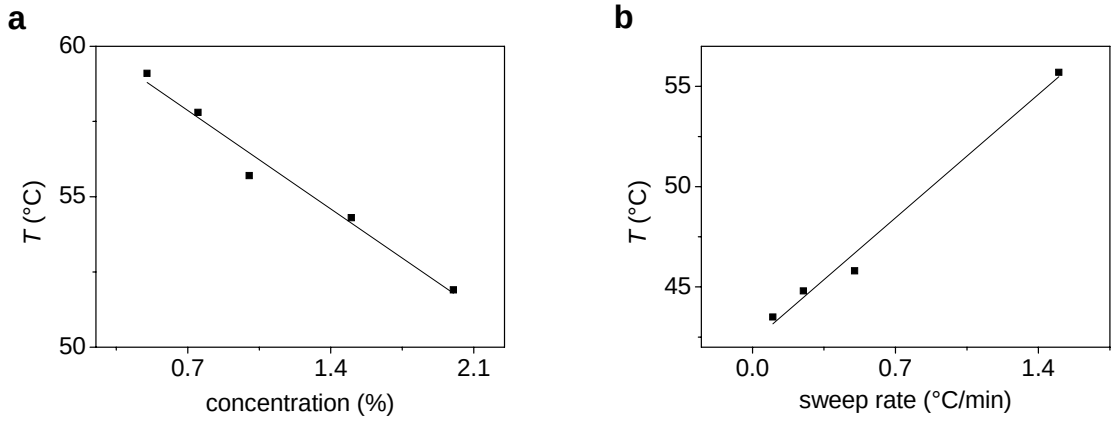

Figure 2. (a) *T*2 *versus* concentration for $M_{1.8}C$ solutions at the sweep rate 1.5°C/min, and (b) *T*2 *versus* sweep rate for a 1 wt% $M_{1.8}C$ solution. The lines are linear fits to the data: (a) *T*2 / °C = 61.1 – 4.7*C* / wt%, (b) *T*2 / °C = 42.3 + 8.8*SR* / (°C/min)

In the case of hydroxypropylmethylcellulose and ethyl(hydroxyethyl)cellulose the viscosity also increases above a temperature *T*2, but it exhibits another transition temperature, *T*1, slightly lower than *T*2, where the viscosity suddenly decreases on increasing the temperature. The typical rheological changes are illustrated in Figure 3a. For HPMC and EHEC, we do not see a clear concentration dependence of *T*1 and *T*2, in contrast to what was found for the *T*2 of MC. The sweep rate, however, is important for the HPMC transition temperatures as shown in Figure 3b. Extrapolation of the data to zero sweep rate gives *T*1 = 56 °C and *T*2 = 61 °C for an $HP_{0.13}M_{1.8}C$ solution and *T*1 = 61 °C and *T*2 = 67 °C for an $HP_{0.12}M_{1.57}C$ solution. The viscosity hysteresis between the heating and cooling curves is smaller for HPMC compared to for MC and even smaller in EHEC, indicating faster aggregation/disaggregation kinetics for HPMC and EHEC than for MC.

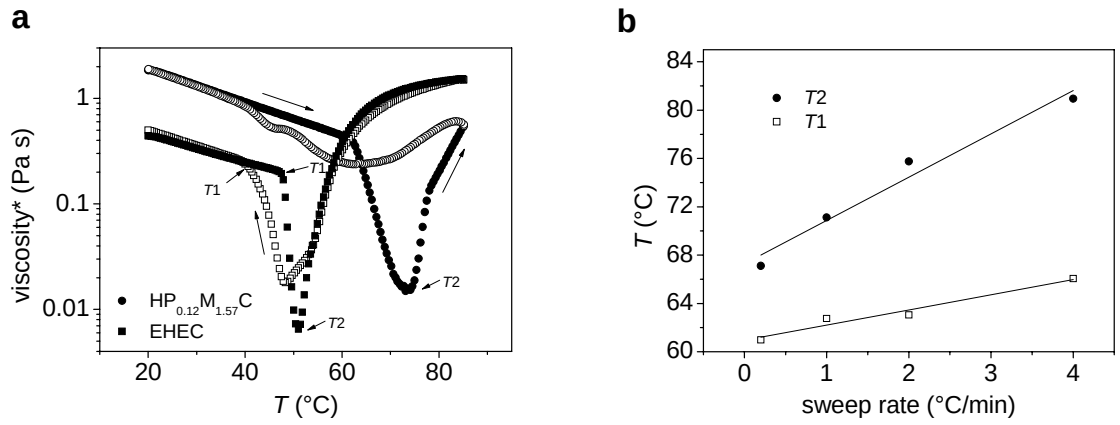

Figure 3. (a) Complex viscosity as a function of temperature (sweep rate 1 °C/min) for 1 wt% aqueous $HP_{0.12}M_{1.57}C$ (circles) and $E_{1.3}HE_{1.5}C$ (squares) solutions. Filled and unfilled symbols correspond to data obtained on heating and cooling, respectively. Arrows along the curve indicate the direction of the temperature sweep. The *T*1 and *T*2 temperatures are also marked. (b) *T*1 and *T*2 *versus* sweep rate for a 0.75 wt% $HP_{0.12}M_{1.57}C$ solution. The lines are linear fits to the data: *T*1 / °C = 60.9 + 1.3*SR* / (°C/min), *T*2 / °C = 67.3 + 3.6*SR* / (°C/min).

The addition of BDG induces a change in the behaviour of MC solutions towards that of the typical HPMC or EHEC solution as illustrated in Figure 4. With a low amount of additive, 2.5 wt% of BDG, a salt-in effect is observed, where the lowest transition temperature, *i.e. T*2, increases. The increase in *T*2 continues on adding more BDG, but with 5 wt% or more of BDG a *T*1 transition point appears just below *T*2. In opposite to *T*2, this transition temperature decreases on adding more BDG and at 10 wt% of BDG it is similar to the *T*2 of the MC in pure water.

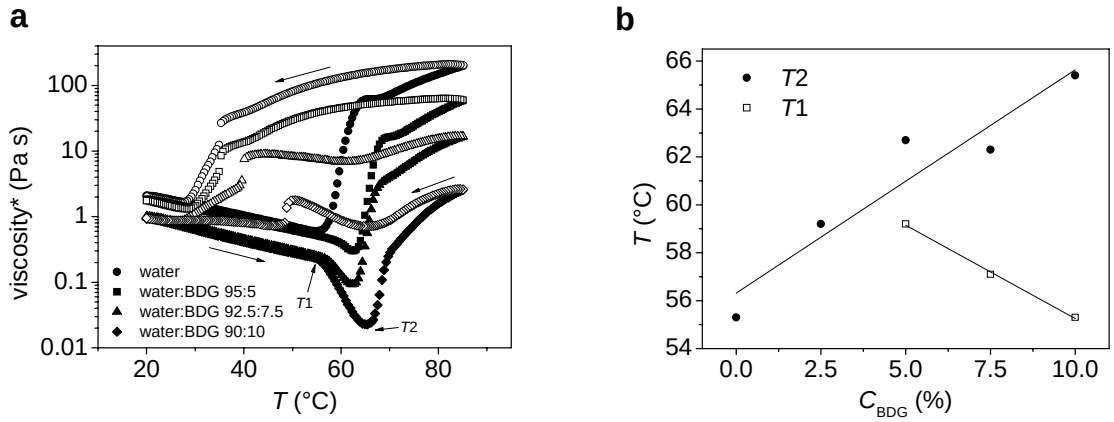

Figure 4. (a) Complex viscosity as a function of temperature (sweep rate 1 °C/min) for 1 wt% $M_{1.6}C$ in water (circles), water/BDG 95:5 (squares), water/BDG 92.5:7.5 (triangles) and water/BDG 90:10 (diamonds). Filled and unfilled symbols correspond to data obtained on heating and cooling, respectively. Arrows along the curve indicate the direction of the temperature sweep. The *T*1 and *T*2 temperatures are also marked. (b) *T*1 and *T*2 temperatures versus BDG concentration for 1 wt% solutions of $M_{1.6}C$. Linear fits are used as guides for the eye.

ii. Aggregation properties

In this work, the aggregation in bulk solution of cellulose ethers, when increasing the temperature in small steps from below to above the transition temperatures, was followed by measurement of the scattered light intensity, using dynamic light scattering. The onset of aggregation is clearly observed in Figure 5a, where the intensity development with increasing temperature is shown for a 0.02 wt% $HP_{0.13}M_{1.8}C$ solution. In a short span starting at 59 °C the increase in intensity is dramatic. The average hydrodynamic diameter, d_h, determined by cumulant analysis with a quadratic fit, increases from around 30 nm to around 300 nm between 59 °C and 60 °C. This increase is closely correlated to the increase in intensity as shown in Figure 5b.

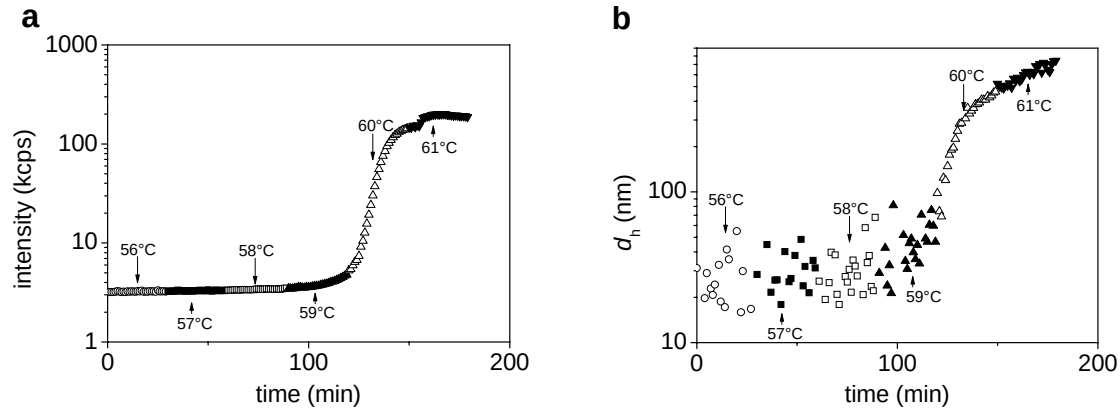

Figure 5. (a) Intensity of scattered light at 90°, and (b) hydrodynamic diameter of the scattering objects in a 0.02 wt% $HP_{0.13}M_{1.8}C$ solution (filtered 0.2 μm).

We have found that the aggregation behaviour shown in Figure 5 is typical for HPMC and EHEC solutions. Figure 6a illustrates this, showing the aggregation of 0.02 wt% $HP_{0.12}M_{1.57}C$ and $E_{1.3}HE_{1.5}C$ aqueous solutions. Methylcelluloses aggregate over a broader temperature range, where the intensity increase is initially slow but gradually increases. This is illustrated for a 0.02 wt% $M_{1.6}C$ aqueous solution in Figure 6a. The onset of aggregation can be approximated to 51-53 °C.

It is found that addition of BDG changes the aggregation behaviour of MC in water to mimic that of HPMC or EHEC in aqueous solutions. Similarly to what was shown in the rheology measurements, a change is induced in the type of transition, when 5 wt% of BDG is added. With 10 wt% of BDG in the MC solution the onset of aggregation is rapid and clearly resembles that of an HPMC in aqueous solution. This is shown in Figure 7. We propose that BDG acts as a physisorbed bulky substituent and thus has a similar effect as the grafted hydroxypropyl groups in HPMC. The hydrodynamic size was in this case determined using the NNLS method, since the solvent induced density fluctuations at lower correlation times.

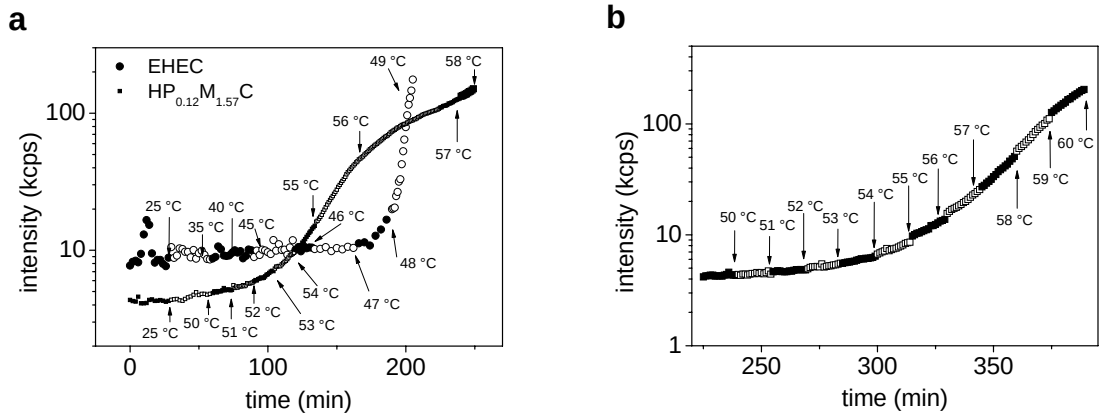

Figure 6. (a) Intensity of light scattered at 90° angle by a 0.02 wt% $E_{1.3}HE_{1.5}C$ aqueous solution (circles) during heating from 25 °C to 49 °C and for a 0.02 wt% $HP_{0.12}M_{1.57}C$ aqueous solution (squares) during heating from 25 °C to 58 °C. (b) Intensity of light (squares) scattered at 90° angle by a 0.02 wt% $M_{1.6}C$ aqueous solution during heating from 50 °C to 60 °C. The scattered light was recorded for around 30 min at each temperature.

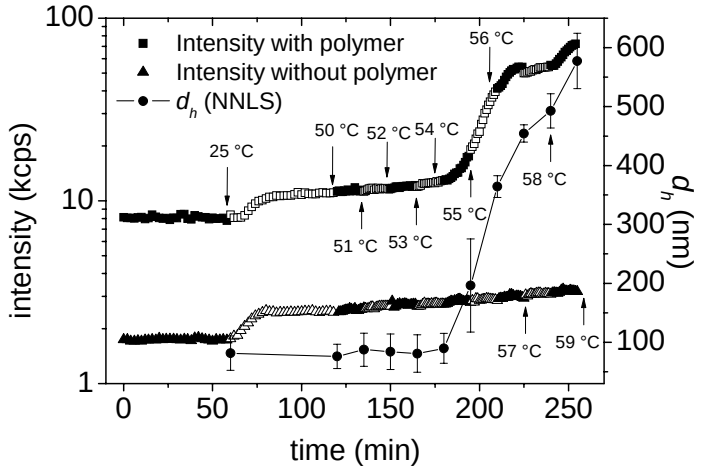

Figure 7. Intensity of light scattered at 90° angle by a 0.02 wt% $M_{1.6}C$ solution in water/BDG 90:10 (squares) and by water/BDG 90:10 (triangles) during heating from 25 °C to 59 °C, and average hydrodynamic diameter (circles with error bars showing the standard deviation) of the scattering objects at each temperature calculated from the Non-Negatively Restricted Least-Squares (NNLS) method.

iii. Aggregation structure

MC and HPMC form very different structures in bulk solution at higher temperatures as shown by Cryo-TEM imaging. Even at low concentrations and at temperatures around the transition points, MC forms fibrillar aggregates, which at a slightly higher temperature assembles into a dense network as shown in Figure 8. This explains the large viscosity increase and gelling. HPMC may also form fibrils (see Figure 9), but due to the bulkiness and hydrophilicity of the hydroxypropyl substituents the structures are more stretched out, and inter-chain connections are less abundant. The networks formed in HPMC solutions do not as readily span the whole solution volume as they do in MC solutions.

Cryo-TEM also shows that the addition of BDG inhibits the formation of fibrils. This is illustrated in Figure 10, where the fibril structure of $M_{1.6}C$ in pure water is compared to the diffuse aggregate structure of the same polymer in a water/BDG 90:10 mixture. These results support the suggestion that BDG acts as a bulky physisorbed substituent.

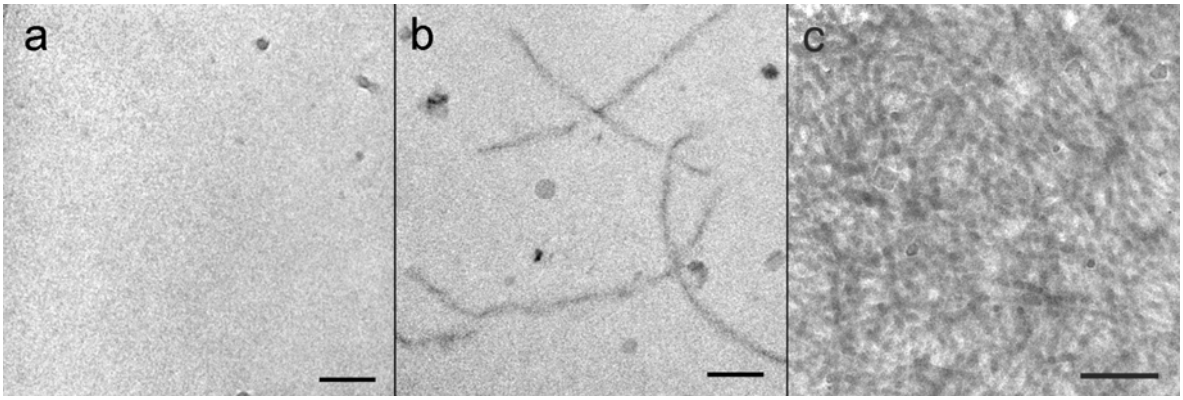

Figure 8. Cryo-TEM images from a $M_{1.8}C$ 0.1 wt% solution at (a-c) 25, 45 and 55°C. Bar = 100 nm (a-b) and 200 nm (c).

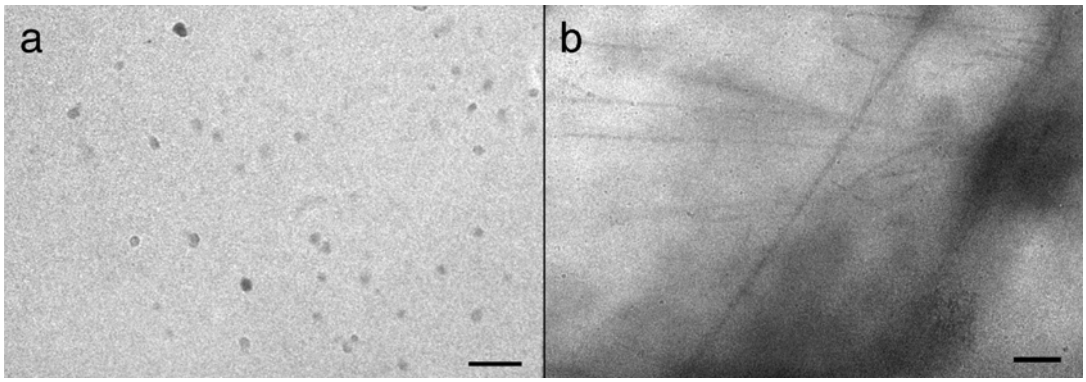

Figure 9. Cryo-TEM images of $HP_{0.13}M_{1.8}C$ solutions. (a) 0.1 wt% solution at 65°C, and (b) 2 wt% solution at 65°C. Bar = 100 nm (a) and 200 nm (b).

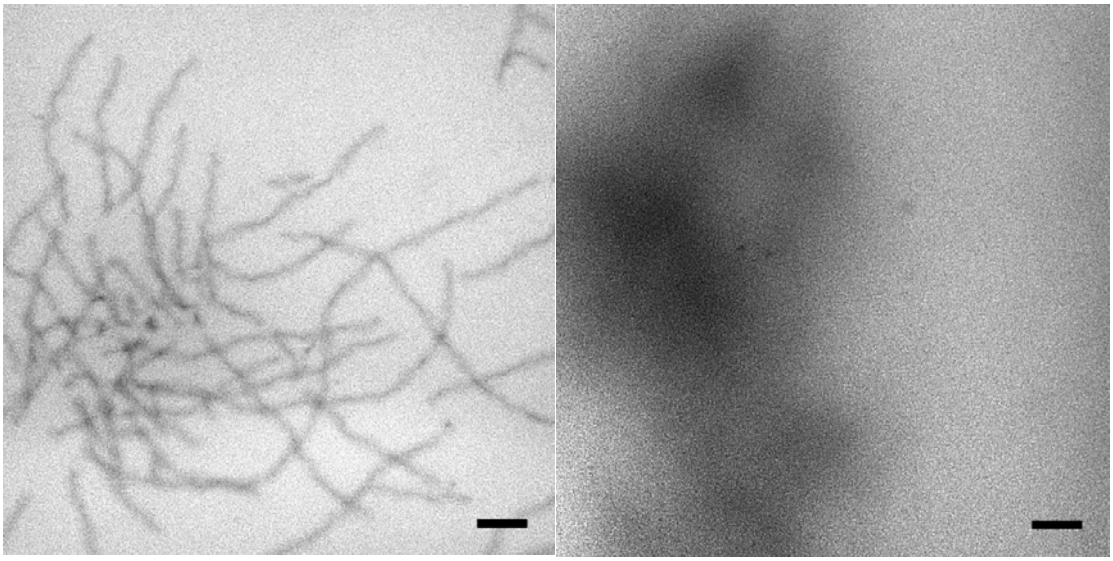

Figure 10. Cryo-TEM image from a 0.02 wt% $M_{1.6}C$ solution in (left) pure water at 60 °C and (right) in a water/BDG 90:10 mixture at 70 °C. Bars = 100 nm.

iv. Bulk transition temperatures

The bulk transition temperatures, obtained from rheology and light scattering measurements, are presented in Table 3. The higher temperature for onset of aggregation found for $HP_{0.13}M_{1.8}C$ compared to $HP_{0.12}M_{1.57}C$ is not expected based on the similarity in hydroxypropyl molar substitution and difference in methoxy degree of substitution. Most likely it is an effect of the larger molecular weight of the latter making the entropy loss on aggregation less significant. However, the viscosity decrease and increase occurs at lower temperatures in $HP_{0.13}M_{1.8}C$ than in $HP_{0.12}M_{1.57}C$. The difference between the aggregation and viscosity experiments is that the former is done at a concentration that is two orders of magnitude lower than in the latter, which, in turn, is due to the requirements of the different techniques.

Table 3. Transition temperatures in aqueous solutions of different cellulose ethers.

Sample	M_w (kDa)	$T1$ (°C)	$T2$ (°C)	Onset of aggregation (°C)
$M_{1.8}C$	160	-	42	42
$HP_{0.13}M_{1.8}C$	70	56	61	60
$HP_{0.21}M_{1.4}C$	ca. 160	75[a]	81[a]	not measured
$M_{1.6}C$	530	-	55[b]	52-53
$M_{1.6}C$ (10 % BDG)	530	55[b]	65[b]	not measured
$HP_{0.12}M_{1.57}C$	620	61	67	52-53
$E_{1.3}HE_{1.5}C$	ca. 300	48[b]	51[b]	48

[a] based on measurement at sweep rate 1.5 °C/min

[b] based on measurement at sweep rate 1 °C/min

c. Interfacial properties

i. Adsorbed amount, thickness and viscoelastic properties

Effect of temperature below T2

MC and HPMC both adsorb significantly on hydrophobized silica (but neither of them on unmodified silica), even at very low concentrations. Changes in adsorbed layers of MC and HPMC were followed using QCM-D and ellipsometry in temperature cycling experiments. When the maximum temperature was below the bulk transition temperatures no large differences were observed between MC and HPMC layers. The adsorbed amount of the polymer is constant if the polymer is removed from the solution before the temperature cycle, but increases with temperature if the surface layer is immersed in polymer solution during the whole experiment as shown for $M_{1.6}C$ in Figure 11.

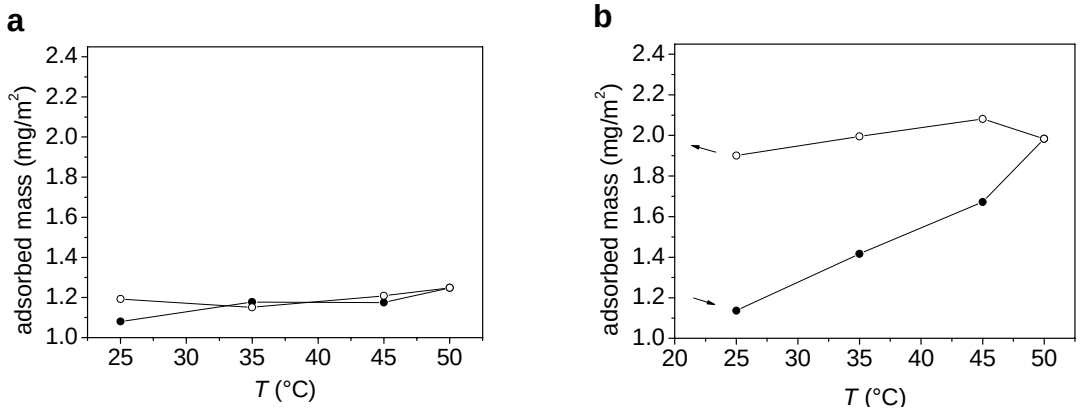

Figure 11. Adsorbed mass (from ellipsometry) as a function of temperature for $M_{1.6}C$ on silanized silica. After adsorption at 25 °C (40 ppm polymer solution), the polymer was (a) rinsed out from the solution, followed by a temperature ramp or (b) kept in the solution during the entire temperature ramp. Filled and unfilled symbols correspond to data obtained on heating and cooling, respectively. At each temperature the data was evaluated after 30-45 min of equilibration. The arrows indicate the direction of the temperature ramp.

The effective thickness of the polymer layers can be calculated from the adsorbed mass (ellipsometry) and the sensed mass (QCM-D), or, alternatively, by Voigt modelling of the QCM-D data. The water content of the layers of MC and HPMC is very high, around 90-95 %, and the effective thickness is close to that calculated with the Voigt model. This is illustrated in Figure 12 for $M_{1.6}C$. The layer viscosity and elasticity, obtained from QCM-D, are shown in Figure 13. It is observed that the pre-adsorbed MC layer immersed in water solution becomes more compact at higher temperature. The change is partly irreversible (over around 24 hours) as the thickness is lower and the elasticity higher after, compared to before, the temperature cycle (Figures 12a and 13a). This effect is more prominent for MC than for HPMC, and not seen in the experiments with the layer immersed in polymer solution (Figures 12b and 13b). The compaction can be rationalized by the stiffness of the MC chain and strong inter-chain contacts. With polymer present in solution during the temperature cycle, additional adsorption masks the temperature effect in the initially adsorbed polymer layer, and the results for MC and HPMC are in this respect similar.

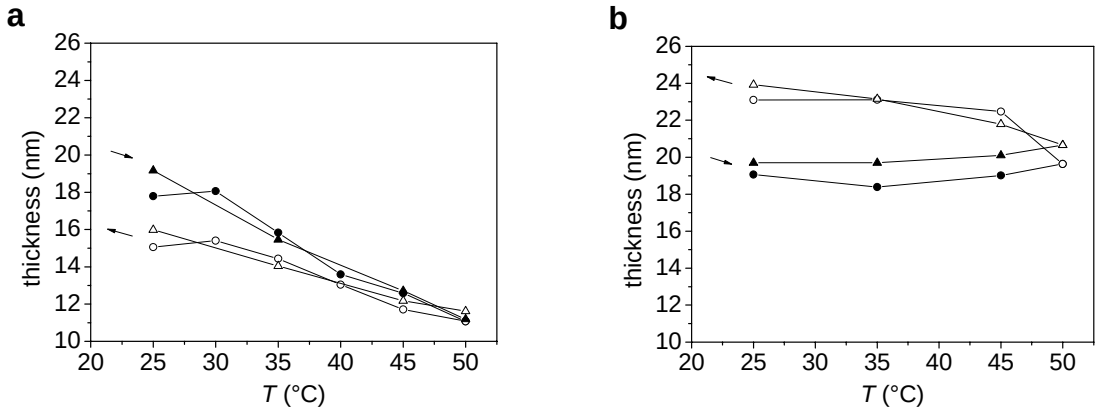

Figure 12. Thickness *versus* temperature obtained from Voigt simulation (circles), and calculated from the sensed and adsorbed mass (triangles), for an adsorbed layer of $M_{1.6}C$ on silanized silica. After adsorption at 25 °C (40 ppm polymer solution), the polymer was (a) rinsed out from the solution, followed by a temperature ramp or (b) kept in the solution during the entire temperature ramp. Filled and unfilled symbols correspond to data obtained on heating and cooling, respectively. At each temperature the data was evaluated after (a) 40 min or (b) 100 min of equilibration. The arrows indicate the direction of the temperature ramp.

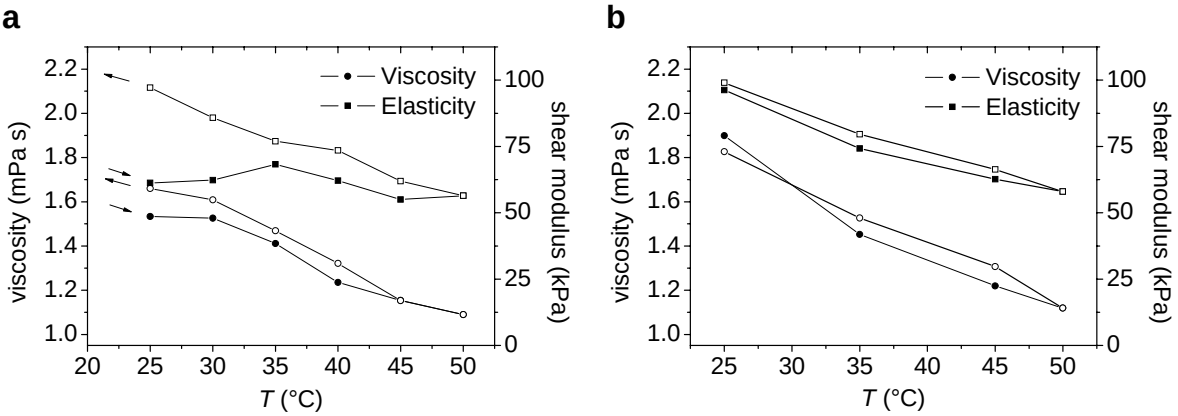

Figure 13. Viscosity and elasticity shear modulus as a function of temperature from Voigt simulation of an adsorbed layer of $M_{1.6}C$ on silanized silica. After adsorption at 25 °C (40 ppm polymer solution), the polymer was (a) rinsed out from the solution, followed by a temperature ramp or (b) kept in the solution during the entire temperature ramp. Filled and unfilled symbols correspond to data obtained on heating and cooling, respectively. At each temperature the data was evaluated after (a) 40 min or (b) 100 min of equilibration. The arrows indicate the direction of the temperature ramp.

Polymer in solution above T2

The adsorbed mass from ellipsometry and in particular the sensed mass from QCM-D increase dramatically in a layer of $HP_{0.12}M_{1.57}C$ above the *T*2 temperature as illustrated in Figure 14, where the data are compared to those obtained in a lower temperature cycle. The layer thickness, water content (Figure 15) and viscoelasticity also undergo significant changes at transition temperatures in the vicinity of *T*2.

In contrast, no similar transitions was observed in a $M_{1.6}C$ layer above its *T*2 temperature. EHEC adsorption (data from literature) increases with increasing temperature at the same rate as HPMC adsorption, when approaching the bulk transition temperature. The adsorbed mass and sensed mass in layers of MC, HPMC and EHEC are compared in Figure 16. The results for HPMC and EHEC in bulk and in surface layers are in line with a recently proposed model on polymer deposition and aggregation,[122] in which it is predicted that deposition on a surface with the same chemistry as the polymer should occur just before aggregation in the solution. This is a consequence of geometrical factors as described by the Derjaguin approximation. The opposite behaviour observed for MC can be related to a stronger tendency for depletion of hydrophobic regions from the layer/solution interface in MC layers compared to HPMC or EHEC layers, which is consistent with the larger tendency of MC to form interconnecting fibrils in bulk solution.

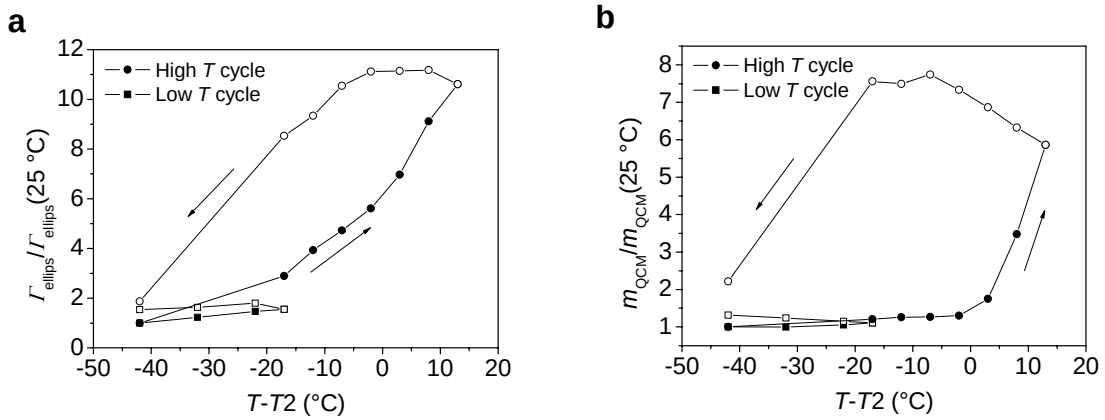

Figure 14. Comparison between two adsorption studies with different maximum temperatures. (a) Adsorbed mass (from ellipsometry) and (b) sensed mass (from Voigt simulation of QCM-D data) for $HP_{0.12}M_{1.57}C$ on silanized silica. The values are normalized by the values acquired at room temperature. The temperatures are relative to the bulk transition temperature, *T*2 = 67 °C. Filled and unfilled symbols correspond to data obtained on heating and cooling, respectively.

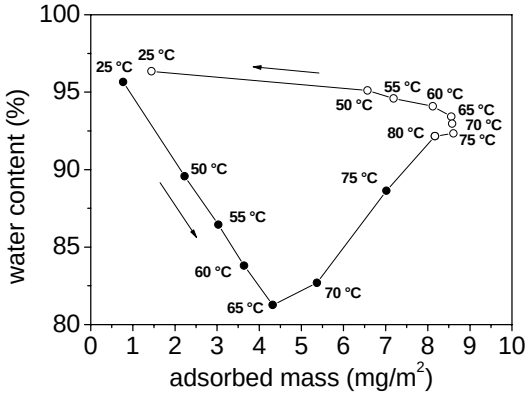

Figure 15. Water content, calculated from the adsorbed mass (ellipsometry) and the sensed mass (QCM-D), *versus* adsorbed mass for an adsorbed layer of $HP_{0.12}M_{1.57}C$ on silanized silica. Filled and unfilled symbols correspond to data obtained on heating and cooling, respectively. The arrows indicate the direction of the temperature ramp.

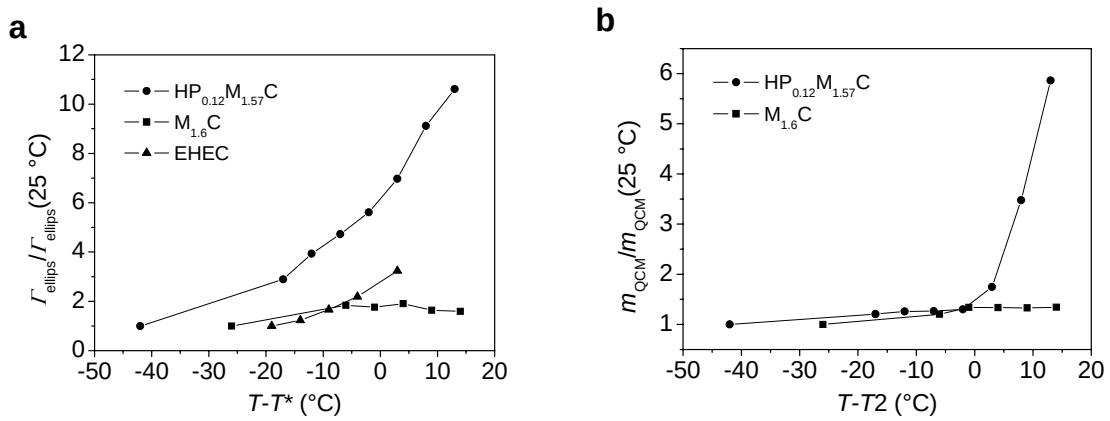

Figure 16. Adsorption of $HP_{0.12}M_{1.57}C$, $M_{1.6}C$ and EHEC on silanized silica as a function of increasing temperature. The data for EHEC is taken from reference:[41] (a) Adsorbed mass (from ellipsometry) for $HP_{0.12}M_{1.57}C$, $M_{1.6}C$ and EHEC and (b) sensed mass (from Voigt simulation of QCM-D data) for $HP_{0.12}M_{1.57}C$ and $M_{1.6}C$. The values for adsorbed and sensed mass are normalized by their values at room temperature. The abscissa is given as T-T*, where for $HP_{0.12}M_{1.57}C$ T*=$T$2=67 °C, for $M_{1.6}C$ T*=$T$2=51 °C; for EHEC T*=T_{cp}=39 °C). The concentration was 40 ppm in the $HP_{0.12}M_{1.57}C$ and $M_{1.6}C$ solutions and 1000 ppm in the EHEC solution. At each temperature the data was evaluated after 70 min of equilibration ($HP_{0.12}M_{1.57}C$ and $M_{1.6}C$) or 90 min (EHEC).

ii. Internal structure of adsorbed MC and HPMC layers on non-polar substrates

The height of the protrusions observed from adsorbed MC and HPMC layers changes with temperature as observed by AFM imaging in PeakForce tapping mode. In Figure 17 the adsorbed layer of $M_{1.6}C$ immersed in polymer solution is shown at three different temperatures. Some adsorption properties of $M_{1.6}C$ are recapitulated in Table 4. It is notisable that the adsorbed amount increases, whereas the layer thickness is close to constant, as the temperature is increased towards the $T$2 transition. This is a consequence of the worsening of the solvent quality of water for these polymers at higher temperature. The aggregates become more abundant but decrease in height, as the $T$2 transition temperature is approached and the solvent quality worsens.

In addition, some regions with fibrillar-like structures are observed in the layer at 25 °C. At 40 °C and higher these structures are distributed over the entire layer. This appearance of aggregates similar to those observed in bulk above 50 °C using Cryo-TEM at a lower temparature in surface layers can be explained by a lower entropic penalty when aggregates are formed on the surface compared to in bulk since a large portion of the conformational (and translational) entropy is lost already during the adsorption process.

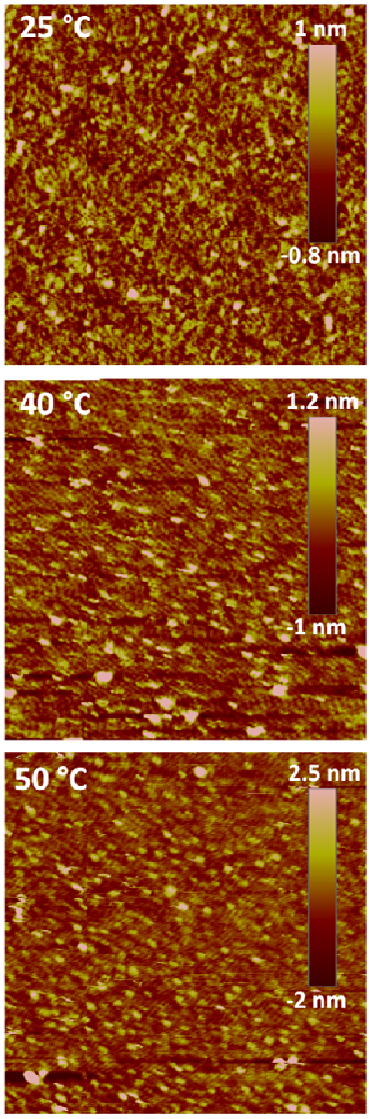

Figure 17. Height images of an adsorbed methylcellulose layer at 25 °C, 40 °C and 50 °C obtained by PeakForce tapping mode AFM operating with a constant feedback peak force of 1nN.

Table 4. Adsorbed layer properties of $M_{1.6}C$ on hydrophobized silica surfaces

Temperature (°C)	Adsorbed amount[a] (mg/m^2)	Sensed mass[b] (mg/m^2)	Layer thickness[c] (nm)	Water content[c] (%)
25	1.1	20	19	94.5
40	1.5*	20*	19	92.6*
50	1.95	21	20	91

[a] Based on ellipsometry measurements reported in Paper III
[b] Based on QCM-D measurements reported in Paper III
[c] Based on QCM-D and ellipsometry measurements reported in Paper III
* Values interpolated from data at 35 °C and 45 °C reported in Paper III

Conclusions

The main conclusions from this thesis work can be summarized in the following points:

- The characteristic viscosity decrease, which occurs in hydroxypropylmethylcellulose (HPMC) and ethyl(hydroxyethyl)cellulose (EHEC) solutions, is likely due to intra-chain contraction and aggregation into less extended structures. An increase in temperature reduces the solvent quality of water for all three polymers, HPMC, EHEC and methylcellulose (MC), inducing an increase in aggregate sizes as observed using light scattering, and an increase in viscosity due to formation of extended structures and, for methylcellulose, closely packed fibrils and networks.
- The aggregation rate follows the order EHEC > HPMC > MC, *i.e.* cellulose ethers containing some bulky and partly hydrophilic substituents assemble into large aggregates more readily than MC. The fibrils in MC also counteract the kinetics of the self-assembly into large aggregates, since the hydrophobic parts of the chain are shielded efficiently from contact with water in the fibrillar structure.
- Addition of 5 wt% BDG to an MC solution induces a viscosity decrease on increasing temperature, typical for HPMC and EHEC. The aggregation rate also increases on adding BDG to resemble the HPMC behaviour in water. With 10 wt% BDG added, MC no longer forms fibrils at elevated temperatures. BDG acts as a physisorbed hydrophilic and bulky substituent on MC, and thus, induces similar constraints on aggregation as the grafted substituents in HPMC and EHEC.
- MC and HPMC adsorb significantly and for practical purposes irreversibly on hydrophobized silica. The adsorbed amount increases with increasing temperature due to the worsening of the solvent quality. Additional adsorption at elevated temperature influences the layer properties significantly, masking the temperature-response of the initially adsorbed polymer layer.
- The water content of the MC and HPMC layers is high as an effect of water entrapment between the stiff polymer chains, which above the transition temperatures also interconnect at a few strong anchoring points. The layers are predominately flat with some protruding polymers or aggregates, which become more abundant at higher temperatures. Fibril-like aggregates form within an adsorbed layer of MC already at 40 °C, significantly lower than the aggregation onset temperature in the bulk solution. This is due to the smaller entropy decrease, compared to the case in bulk solution, since a large portion of the conformational entropy is lost during adsorption.
- In HPMC layers, around the bulk transition temperatures and higher, the increase in adsorbed mass and the changes in layer properties are dramatic. In contrast, for MC, bulk aggregation is favoured over deposition. MC layers may have a more significant depletion of hydrophobic regions from the layer–solution interface compared to the HPMC or EHEC layers.
- In MC layers, the normal surface forces are rather insensitive to temperature, due to accumulation of the hydrophobic groups within the layer, and further shielding of these groups by formation of fibrillar structures at higher temperatures. The friction forces change significantly with increasing temperature. At low loads the friction increases with increasing temperature due to increasing attraction between segments within the surface layer. At high loads the friction decreases with increasing temperature, due to a higher load bearing capacity. This is caused by the worsening of the solvent quality, which results in stronger polymer–surface affinity and better cohesion within the layer.
- The equilibration time for bulk changes is slow, as illustrated by a large difference in viscosity on cooling compared to on heating, particularly for MC. The adsorption hysteresis is significant during heat treatment for both MC and HPMC. For each temperature change, the adsorption process needed a long time to reach equilibrium, particularly upon cooling. Thus, the properties are dominated by long-lived kinetically trapped states rather than equilibrium states.

References

1. Schmaljohann, D., Thermo- and pH-responsive polymers in drug delivery. *Advanced Drug Delivery Reviews* **2006,** *58* (15), 1655-1670.
2. Chu, L. Y.; Niitsuma, T.; Yamaguchi, T.; Nakao, S., Thermoresponsive transport through porous membranes with grafted PNIPAM gates. *Aiche Journal* **2003,** *49* (4), 896-909.
3. Bilbao-Sainz, C.; Wood, R.; Williams, T. G.; McHugh, T. H., Composite Edible Films Based on Hydroxypropyl Methylcellulose Reinforced with Microcrystalline Cellulose Nanoparticles. *J. Agric. Food Chem.* **2010,** *58* (6), 3753-3760.
4. Franks, G. V.; Li, H. H.; O'Shea, J. P.; Qiao, G. G., Temperature responsive polymers as multiple function reagents in mineral processing. *Adv. Powder Technol.* **2009,** *20* (3), 273-279.
5. Urban, M. W., Intelligent Polymeric Coatings; Current and Future Advances. *Polymer Reviews* **2006,** *46* (4), 329 - 339.
6. Hart, D. S.; Gehrke, S. H., Thermally associating polypeptides designed for drug delivery produced by genetically engineered cells. *Journal Of Pharmaceutical Sciences* **2007,** *96* (3), 484-516.
7. Dedinaite, A.; Thormann, E.; Olanya, G.; Claesson, P. M.; Nystrom, B.; Kjoniksen, A. L.; Zhu, K. Z., Friction in Aqueous Media Tuned by Temperature-Responsive Polymer Layers. *Soft Matter* **2010,** *6* (11), 2489-2498.
8. Zhu, P. W.; Napper, D. H., Experimental Observation of Coil-to-Globule Type Transitions at Interfaces. *Journal of Colloid and Interface Science* **1994,** *164* (2), 489.
9. Acciaro, R.; Aulin, C.; Wagberg, L.; Lindstrom, T.; Claesson, P. M.; Varga, I., Investigation of the formation, structure and release characteristics of self-assembled composite films of cellulose nanofibrils and temperature responsive microgels. *Soft Matter* **2011,** *7* (4), 1369-1377.
10. O'Shea, J. P.; Qiao, G. G.; Franks, G. V., Solid-liquid separations with a temperature-responsive polymeric flocculant: Effect of temperature and molecular weight on polymer adsorption and deposition. *J. Colloid Interface Sci.* **2010,** *348* (1), 9-23.
11. Schild, H. G., Poly(N-isopropylacrylamide): experiment, theory and application. *Prog. Polym. Sci.* **1992,** *17* (2), 163.
12. Morimoto, N.; Obeid, R.; Yamane, S.; Winnik, F. M.; Akiyoshi, K., Composite nanomaterials by self-assembly and controlled crystallization of poly(2-isopropyl-2-oxazoline)-grafted polysaccharides. *Soft Matter* **2009,** *5* (8), 1597-1600.
13. Saigal, T.; Dong, H. C.; Matyjaszewski, K.; Tilton, R. D., Pickering Emulsions Stabilized by Nanoparticles with Thermally Responsive Grafted Polymer Brushes. *Langmuir* **2010,** *26* (19), 15200-15209.
14. Verbrugghe, S.; Bernaerts, K.; Prez, F. E. D., Thermo-Responsive and Emulsifying Properties of Poly(<I>N</I>-vinylcaprolactam) Based Graft Copolymers. *Macromolecular Chemistry and Physics* **2003,** *204* (9), 1217-1225.
15. Kawaguchi, S.; Imai, G.; Suzuki, J.; Miyahara, A.; Kitano, T., Aqueous solution properties of oligo- and poly(ethylene oxide) by static light scattering and intrinsic viscosity. *Polymer* **1997,** *38* (12), 2885-2891.
16. Thormann, E.; Claesson, P. M.; Mouritsen, O. G., Tuning structural forces between silica surfaces by temperature-induced micellization of responsive block copolymers. *Physical Chemistry Chemical Physics* **2010,** *12* (36), 10730-10735.
17. Clasen, C.; Kulicke, W. M., Determination of viscoelastic and rheo-optical material functions of water-soluble cellulose derivatives. *Prog. Polym. Sci.* **2001,** *26* (9), 1839-1919.
18. Nakagawa, A.; Fenn, D.; Koschella, A.; Heinze, T.; Kamitakahara, H., Physical Properties of Diblock Methylcellulose Derivatives with Regioselective Functionalization Patterns: First Direct Evidence that a Sequence of 2,3,6-Tri-O-methyl-glucopyranosyl Units Causes Thermoreversible Gelation of Methylcellulose. *J. Polym. Sci. Pt. B-Polym. Phys.* **2011,** *49* (21), 1539-1546.

19. Nakagawa, A.; Fenn, D.; Koschella, A.; Heinze, T.; Kamitakahara, H., Synthesis of Diblock Methylcellulose Derivatives with Regioselective Functionalization Patterns. *J. Polym. Sci. Pol. Chem.* **2011,** *49* (23), 4964-4976.
20. Ibbett, R. N.; Philp, K.; Price, D. M., 13C n.m.r. studies of the thermal behaviour of aqueous solutions of cellulose ethers. *Polymer* **1992,** *33* (19), 4087-94.
21. Ruel-Gariepy, E.; Leroux, J.-C., In situ-forming hydrogels--review of temperature-sensitive systems. *European Journal of Pharmaceutics and Biopharmaceutics* **2004,** *58* (2), 409-426.
22. Lin, S. Y.; Wang, S. L.; Wei, Y. S.; Li, M. J., Temperature effect on water desorption from methylcellulose films studied by thermal FT-IR micro spectroscopy. *Surf. Sci.* **2007,** *601* (3), 781-785.
23. Perez, O. E.; Sanchez, C. C.; Pilosof, A. M. R.; Patino, J. M. R., Dynamics of adsorption of hydroxypropyl methylcellulose at the air-water interface. *Food Hydrocolloids* **2008,** *22* (3), 387-402.
24. Chen, C. H.; Tsai, C. C.; Chen, W.; Mi, F. L.; Liang, H. F.; Chen, S. C.; Sung, H. W., Novel Living Cell Sheet Harvest System Composed of Thermoreversible Methylcellulose Hydrogels. *Biomacromolecules* **2006,** *7* (3), 736-743.
25. Karlson, L. Hydrophobically Modified Polymers - Rheology and Molecular Associations. Lund University, Lund, 2002.
26. Takeuchi, M.; Kageyama, S.; Suzuki, H.; Wada, T.; Notsu, Y.; Ishii, F., Rheological properties of reversible thermo-setting in situ gelling solutions with the methylcellulose–polyethylene glycol–citric acid ternary system. *Colloid & Polymer Science* **2003,** *281* (12), 1178.
27. Rajabi-Siahboomi, A. R.; Bowtell, R. W.; Mansfield, P.; Henderson, A.; Davies, M. C.; Melia, C. D., Structure and behaviour in hydrophilic matrix sustained release dosage forms: 2. NMR-imaging studies of dimensional changes in the gel layer and core of HPMC tablets undergoing hydration. *Journal of Controlled Release* **1994,** *31* (2), 121.
28. Sanz, T.; Fernandez, M. A.; Salvador, A.; Munoz, J.; Fiszman, S. M., Thermogelation properties of methylcellulose (MC) and their effect on a batter formula. *Food Hydrocolloids* **2005,** *19* (1), 141.
29. Rasenack, N.; Hartenhauer, H.; Muller, B. W., Microcrystals for dissolution rate enhancement of poorly water-soluble drugs. *International Journal of Pharmaceutics* **2003,** *254* (2), 137-145.
30. Stabenfeldt, S. E.; Garcia, A. J.; LaPlaca, M. C., Thermoreversible laminin-functionalized hydrogel for neural tissue engineering. *Journal of Biomedical Materials Research, Part A* **2006,** *77A* (4), 718-725.
31. Yin, Y. M.; Zhang, H. B.; Nishinari, K., Voltammetric characterization on the hydrophobic interaction in polysaccharide hydrogels. *Journal Of Physical Chemistry B* **2007,** *111* (7), 1590-1596.
32. Baumgartner, S.; Planinsekc, O.; Srcic, S.; Kristl, J., Analysis of surface properties of cellulose ethers and drug release from their matrix tablets. *European Journal of Pharmaceutical Sciences* **2006,** *27* (4), 375-383.
33. Claesson, P. M.; Malmsten, M.; Lindman, B., Forces between Hydrophobic Surfaces Coated with Ethyl(Hydroxyethyl)Cellulose in the Presence of an Ionic Surfactant. *Langmuir* **1991,** *7* (7), 1441-1446.
34. Elam, J. H.; Karlsson, C.; Nygren, H., PRE-ADSORPTION OF A CELLULOSE ETHER ONTO POLYMER SURFACES - ADSORPTION OF ADHESINS AND PLATELET ACTIVATION. *Biomaterials* **1993,** *14* (3), 233-237.
35. Joabsson, F.; Thuresson, K.; Lindman, B., Interfacial interaction between cellulose derivatives and surfactants at solid surfaces. An ellipsometry study. *Langmuir* **2001,** *17* (5), 1499-1505.
36. Karlson, L.; Joabsson, F.; Thuresson, K., Phase behavior and rheology in water and in model paint formulations thickened with HM-EHEC: influence of the chemical structure and the distribution of hydrophobic tails. *Carbohydrate Polymers* **2000,** *41* (1), 25-35.
37. Karlsson, C.; Braide, M.; Nygren, H., Interactions between whole blood and foreign materials: surface-adsorbed cellulose ethers reduce granulocyte activation by inflammatory mediators. *Colloids and Surfaces B - Biointerfaces* **2000,** *17* (2), 95-101.
38. Karlsson, C.; Carlsson, A.; Stenberg, M.; Nygren, H., COOPERATIVITY IN THE ADSORPTION OF CELLULOSE ETHERS AND FIBRINOGEN AT LIQUID-SOLID INTERFACES. *Colloid Polym. Sci.* **1992,** *270* (4), 377-383.

39. Malmsten, M.; Claesson, P. M., Temperature-dependent adsorption and surface forces in aqueous ethyl(hydroxyethyl)cellulose solutions. *Langmuir* **1991,** *7* (5), 988-994.
40. Malmsten, M.; Claesson, P. M.; Pezron, E.; Pezron, I., Temperature-dependent forces between hydrophobic surfaces coated with ethyl(hydroxyethyl)cellulose. *Langmuir* **1990,** *6* (10), 1572-1578.
41. Malmsten, M.; Lindman, B., Ellipsometry studies of the adsorption of cellulose ethers. *Langmuir* **1990,** *6* (2), 357-364.
42. Pezron, I.; Pezron, E.; Claesson, P. M.; Malmsten, M., Temperature-dependent forces between hydrophilic mica surfaces coated with ethyl(hydroxyethyl)cellulose. *Langmuir* **1991,** *7* (10), 2248-2252.
43. Carlsson, A.; Karlstrom, G.; Lindman, B., Thermal gelation of nonionic cellulose ethers and ionic surfactants in water. *Colloids and Surfaces* **1990,** *47*, 147.
44. Dahlvik, P.; Lason, L., A comparison of two cellulosic thickeners in coating colors at different temperatures: flow behavior and coating performance. *Paperi Ja Puu-Paper And Timber* **2001,** *83* (7), 542-547.
45. Djuve, J.; Grant, L. M.; Sjoblom, J.; Goloub, T. P.; Pugh, R. J., Templating of ethyl(hydroxyethyl)cellulose on graphite by surfactant-polymer interactions. *Langmuir* **2002,** *18* (7), 2673-2677.
46. Egermayer, M.; Karlberg, M.; Piculell, L., Gels of hydrophobically modified ethyl (hydroxyethyl) cellulose cross-linked by amylose: Effects of hydrophobe architecture. *Langmuir* **2004,** *20* (6), 2208-2214.
47. Kjoniksen, A. L.; Knudsen, K. D.; Nystrom, B., Phase separation and structural properties of semidilute aqueous mixtures of ethyl(hydroxyethyl)cellulose and an ionic surfactant. *European Polymer Journal* **2005,** *41* (9), 1954-1964.
48. Persson, B.; Nilsson, S.; Sundelof, L. O., On the characterization principles of some technically important water-soluble nonionic cellulose derivatives .2. Surface tension and interaction with a surfactant. *Carbohydrate Polymers* **1996,** *29* (2), 119-127.
49. Singh, S. K.; Nilsson, S., Thermodynamics of interaction between some cellulose ethers and SDS by titration microcalorimetry - I. EHEC and HPMC. *J. Colloid Interface Sci.* **1999,** *213* (1), 133-151.
50. Um, S. U.; Poptoshev, E.; Pugh, R. J., Aqueous solutions of ethyl (hydroxyethyl) cellulose and hydrophobic modified ethyl (hydroxyethyl) cellulose polymer: Dynamic surface tension measurements. *J. Colloid Interface Sci.* **1997,** *193* (1), 41-49.
51. Joabsson, F.; Rosen, O.; Thuresson, K.; Piculell, L.; Lindman, B., Phase behavior of a "Clouding" nonionic polymer in water. Effects of hydrophobic modification and added surfactant on phase compositions. *Journal Of Physical Chemistry B* **1998,** *102* (16), 2954-2959.
52. Scherlund, M.; Brodin, A.; Malmsten, M., Nonionic cellulose ethers as potential drug delivery systems for periodontal anesthesia. *J. Colloid Interface Sci.* **2000,** *229* (2), 365-374.
53. Bohic, S.; Weiss, P.; Roger, P.; Daculsi, G., Light scattering experiments on aqueous solutions of selected cellulose ethers: contribution to the study of polymer-mineral interactions in a new injectable biomaterial. *Journal of Materials Science - Materials in Medicine* **2001,** *12* (3), 201-205.
54. Ohta, K. M.; Fuji, M.; Takei, T.; Chikazawa, M., Development of a simple method for the preparation of a silica gel based controlled delivery system with a high drug content. *European Journal of Pharmaceutical Sciences* **2005,** *26* (1), 87.
55. Sarkar, N., Thermal gelation properties of methyl and hydroxypropyl methylcellulose. *Journal of Applied Polymer Science* **1979,** *24* (4), 1073-1087.
56. Kobayashi, K.; Huang, C. I.; Lodge, T. P., Thermoreversible gelation of aqueous methylcellulose solutions. *Macromolecules* **1999,** *32* (21), 7070-7077.
57. Schupper, N.; Rabin, Y.; Rosenbluh, M., Multiple stages in the aging of a physical polymer gel. *Macromolecules* **2008,** *41* (11), 3983-3994.
58. Desbrieres, J.; Hirrien, M.; Rinaudo, M., A calorimetric study of methylcellulose gelation. *Carbohydrate Polymers* **1998,** *37* (2), 145-152.
59. Hirrien, M.; Desbrieres, J.; Rinaudo, M., Physical properties of methylcelluloses in relation with the conditions for cellulose modification. *Carbohydrate Polymers* **1996,** *31* (4), 243-252.

60. Li, L.; Wang, Q. Q.; Xu, Y. R., Thermoreversible association and gelation of methylcellulose in aqueous solutions. *Nihon Reoroji Gakkaishi* **2003,** *31* (5), 287-296.
61. Haque, A.; Morris, E. R., Thermogelation of methylcellulose. Part I: molecular structures and processes. *Carbohydrate Polymers* **1993,** *22* (3), 161-173.
62. Kato, T.; Yokoyama, M.; Takahashi, A., Melting temperatures of thermally reversible gels IV. Methyl cellulose-water gels. *Colloid and Polymer Science* **1978,** *256* (1), 15-21.
63. Sarkar, N.; Walker, L. C., Hydration Dehydration Properties Of Methylcellulose And Hydroxypropylmethylcellulose. *Carbohydrate Polymers* **1995,** *27* (3), 177-185.
64. Yuguchi, Y.; Urakawa, H.; Kitamura, S.; Ohno, S.; Kajiwara, K., Gelation Mechanism Of Methylhydroxypropylcellulose In Aqueous-Solution. *Food Hydrocolloids* **1995,** *9* (3), 173-179.
65. Nishinari, K.; Hofmann, K. E.; Kohyama, K.; Nishinari, N., Gel-sol transition of methylcellulose. *Macromolecular Chemistry And Physics* **1997,** *198* (4), 1217-1226.
66. Chandler, D., Interfaces and the driving force of hydrophobic assembly. *Nature* **2005,** *437* (7059), 640-647.
67. Lum, K.; Chandler, D.; Weeks, J. D., Hydrophobicity at Small and Large Length Scales. *Journal of Physical Chemistry B* **1999,** *103* (22), 4570-4577.
68. Tanford, C., *The hydrophobic effect: formation of micelles and biological membranes*. Wiley: New York, 1973.
69. Li, L., Thermal gelation of methylcellulose in water: Scaling and thermoreversibility. *Macromolecules* **2002,** *35* (15), 5990-5998.
70. Faroongsarng, D.; Sukonrat, P., Thermal behavior of water in the selected starch- and cellulose-based polymeric hydrogels. *International Journal of Pharmaceutics* **2008,** *352* (1-2), 152-158.
71. Nokhodchi, A.; Ford, J. L.; Rubinstein, M. H., Studies on the interaction between water and (hydroxypropyl)methylcellulose. *Journal of Pharmaceutical Sciences* **1997,** *86* (5), 608-615.
72. McCrystal, C. B.; Ford, J. L.; He, R.; Craig, D. Q. M.; Rajabi-Siahboomi, A. R., Characterisation of water behaviour in cellulose ether polymers using low frequency dielectric spectroscopy. *International Journal of Pharmaceutics* **2002,** *243* (1-2), 57-69.
73. Sammon, C.; Bajwa, G.; Timmins, P.; Melia, C. D., The application of attenuated total reflectance Fourier transform infrared spectroscopy to monitor the concentration and state of water in solutions of a thermally responsive cellulose ether during gelation. *Polymer* **2006,** *47* (2), 577-584.
74. Buslov, D. K.; Sushko, N. I.; Tretinnikov, O. N., Study Of Thermal Gelation Of Methylcellulose In Water Using Ftir-Atr Spectroscopy. *J. Appl. Spectrosc.* **2008,** *75* (4), 514-518.
75. Sekiguchi, Y.; Sawatari, C.; Kondo, T., A gelation mechanism depending on hydrogen bond formation in regioselectively substituted O-methylcelluloses. *Carbohydrate Polymers* **2003,** *53* (2), 145-153.
76. Chevillard, C.; Axelos, M. A. V., Phase separation of aqueous solution of methylcellulose. *Colloid and Polymer Science* **1997,** *275* (6), 537-545.
77. Tanaka, F., Phase formation of associating polymers: Gelation, phase separation and microphase formation. *Advances in Colloid and Interface Science* **1996,** *63*, 23-40.
78. Tanaka, F.; Ishida, M., Thermoreversible Gelation Of Hydrated Polymers. *Journal of the Chemical Society, Faraday Transactions* **1995,** *91* (16), 2663-2670.
79. Joshi, S. C.; Lam, Y. C.; Bin, C., Modelling leading to water entrapment point in thermally driven hydrogelation of methyl cellulose. *e-Polymers* **2008**.
80. Sarkar, N., Kinetics Of Thermal Gelation Of Methylcellulose And Hydroxypropylmethylcellulose In Aqueous-Solutions. *Carbohydrate Polymers* **1995,** *26* (3), 195-203.
81. Silva, S. M. C.; Pinto, F. V.; Antunes, F. E.; Miguel, M. G.; Sousa, J. J. S.; Pais, A., Aggregation and gelation in hydroxypropylmethyl cellulose aqueous solutions. *J. Colloid Interface Sci.* **2008,** *327* (2), 333-340.
82. Csoka, G.; Marton, S.; Gelencser, A.; Klebovich, I., Thermoresponsive properties of different cellulose derivatives. *European Journal of Pharmaceutical Sciences* **2005,** *25*, S74-S75.
83. Hussain, S.; Keary, C.; Craig, D. Q. M., A thermorheological investigation into the gelation and phase separation of hydroxypropyl methylcellulose aqueous systems. *Polymer* **2002,** *43* (21), 5623-5628.

84. Onoda-Yamamuro, N.; Yamamuro, O.; Inamura, Y.; Nomura, H., QENS study on thermal gelation in aqueous solution of methylcellulose. *Physica B* **2007,** *393* (1-2), 158-160.
85. Ibbett, R. N.; Philp, K.; Price, D. M., 13C n.m.r. Studies of the Thermal Behaviour of Aqueous Solutions of Cellulose Ethers. *Polymer* **1992,** *33* (19), 4087-4094.
86. Haque, A.; Richardson, R. K.; Morris, E. R.; Gidley, M. J.; Caswell, D. C., Thermogelation of methylcellulose. Part II: effect of hydroxypropyl substituents. *Carbohydrate Polymers* **1993,** *22* (3), 175-186.
87. Zhang, Y. J.; Furyk, S.; Bergbreiter, D. E.; Cremer, P. S., Specific ion effects on the water solubility of macromolecules: PNIPAM and the Hofmeister series. *Journal of the American Chemical Society* **2005,** *127* (41), 14505-14510.
88. *Glycol Ethers*. Dow Chemical Company, USA: 2001.
89. Smith, S.; Wiseman, P.; Boudreau, L.; Marangoni, G.; Palepu, R., Effect of microheterogeneity on bulk and surface properties of binary mixtures of polyoxyethene glycol monobutyl ethers with water. *Journal of Solution Chemistry* **1994,** *23* (2), 207-222.
90. Thuresson, K.; Nilsson, S.; Lindman, B., Influence of Cosolutes on Phase Behavior and Viscosity of a Nonionic Cellulose Ether. The Effect of Hydrophobic Modification. *Langmuir* **1996,** *12* (10), 2412-2417.
91. Courtenay, E. S.; Capp, M. W.; Record, M. T., Thermodynamics of interactions of urea and guanidinium salts with protein surface: Relationship between solute effects on protein processes and changes in water-accessible surface area. *Protein Science* **2001,** *10* (12), 2485-2497.
92. Fleer, G. J.; Cohen Stuart, M. A.; Scheutjens, J. M. H. M.; Cosgrove, T.; Vincent, B., *Polymers at Interfaces*. Chapman & Hall: London, 1993.
93. Jhon, Y. K.; Bhat, R. R.; Jeong, C.; Rojas, O. J.; Szleifer, I.; Genzer, J., Salt-induced Depression of Lower Critical Solution Temperature in a Surface-grafted Neutral Thermoresponsive Polymer. *Macromolecular Rapid Communications* **2006,** *27* (9), 697-701.
94. Liu, G. M.; Zhang, G. Z., Collapse and swelling of thermally sensitive Poly(N-isopropylacrylamide) brushes monitored with a quartz crystal microbalance. *Journal of Physical Chemistry B* **2005,** *109* (2), 743-747.
95. Plunkett, M. A.; Wang, Z.; Rutland, M. W.; Johannsmann, D., Adsorption of pNIPAM layers on hydrophobic gold surfaces, measured in situ by QCM and SPR. *Langmuir* **2003,** *19* (17), 6837-6844.
96. Zhang, G. Z., Study on conformation change of thermally sensitive linear grafted poly(N-isopropylacrylamide) chains by quartz crystal microbalance. *Macromolecules* **2004,** *37* (17), 6553-6557.
97. Perez, O. E.; Sanchez, C. C.; Patino, J. M. R.; Pilosof, A. M. R., Thermodynamic and dynamic characteristics of hydroxypropylmethylcellulose adsorbed films at the air-water interface. *Biomacromolecules* **2006,** *7* (1), 388-393.
98. Schmitz, K. S., *An Introduction to Dynamic Light Scattering by Macromolecules*. Academic Press: London, 1990.
99. Brown, J. C.; Pusey, P. N., Measurement of diffusion coefficients of polydisperse solutes by photon correlation spectroscopy. *Journal of Physics D: Applied Physics* **1974,** *7* (2), L31.
100. Halthur, T. J.; Arnebrant, T.; Macakova, L.; Feiler, A., Sequential Adsorption of Bovine Mucin and Lactoperoxidase to Various Substrates Studied with Quartz Crystal Microbalance with Dissipation. *Langmuir* **2010,** *26* (7), 4901-4908.
101. Sauerbrey, G., Verwendung von Schwingquarzen zur Wägung dünner Schichten und zur Mikrowägung. *Zeitschrift für Physik* **1959,** *155*, 206-222.
102. Hook, F.; Rodahl, M.; Kasemo, B.; Brzezinski, P., Structural Changes in Hemoglobin during Adsorption to Solid Surfaces: Effects of pH, Ionic Strength, and Ligand Binding. *Proceedings of the National Academy of Sciences, USA* **1998,** *95* (21), 12271-12276.
103. Rodahl, M.; Kasemo, B., On the measurement of thin liquid overlayers with the quartz-crystal microbalance. *Sens. Actuator A-Phys.* **1996,** *54* (1-3), 448-456.
104. Voinova, M. V.; Rodahl, M.; Jonson, M.; Kasemo, B., Viscoelastic acoustic response of layered polymer films at fluid-solid interfaces: Continuum mechanics approach. *Phys. Scr.* **1999,** *59* (5), 391-396.

105. Iruthayaraj, J.; Olanya, G.; Claesson, P. M., Viscoelastic Properties of Adsorbed Bottle-Brush Polymer Layers Studied by Quartz Crystal Microbalance - Dissipation Measurements. *J. Phys. Chem. C* **2008,** *112* (38), 15028-15036.
106. Landgren, M.; Joensson, B., Determination of the optical properties of silicon/silica surfaces by means of ellipsometry, using different ambient media. *Journal of Physical Chemistry* **1993,** *97* (8), 1656-1660.
107. McCrackin, F. L., Steinberg, H. L., Stromberg, R. R., Passaglia, E., Measurement of the Thickness and Refractive Index of Very Thin Films and the Optical Properties of Surfaces by Ellipsometry. *Journal of Research of the National Bureau of Standards* **1963,** *67A* (4), 363-377.
108. Cuypers, P. A.; Corsel, J. W.; Janssen, M. P.; Kop, J. M. M.; Hermens, W. T.; Hemker, H. C., The Adsorption of Prothrombin to Phosphatidylserine Multilayers Quantitated by Ellipsometry. *J. Biol. Chem.* **1983,** *258* (4), 2426-2431.
109. Feijter, J. A. D.; Benjamins, J.; Veer, F. A., Ellipsometry as a tool to study the adsorption behavior of synthetic and biopolymers at the air-water interface. *Biopolymers* **1978,** *17* (7), 1759-1772.
110. Larsson, C.; Rodahl, M.; Hook, F., Characterization of DNA immobilization and subsequent hybridization on a 2D arrangement of streptavidin on a biotin-modified lipid bilayer supported on SiO2. *Anal. Chem.* **2003,** *75* (19), 5080-5087.
111. *Methocel Cellulose Ethers Technical Handbook*. Dow Chemical Company, USA: 2002.
112. Zaera, F., Surface chemistry at the liquid/solid interface. *Surf. Sci.* **2011,** *605* (13-14), 1141-1145.
113. Burdukova, E.; Li, H. H.; Ishida, N.; O'Shea, J. P.; Franks, G. V., Temperature controlled surface hydrophobicity and interaction forces induced by poly (N-isopropylacrylamide). *J. Colloid Interface Sci.* **2010,** *342* (2), 586-592.
114. Wang, G.; Rodahl, M.; Edvardsson, M.; Svedhem, S.; Ohlsson, G.; Hook, F.; Kasemo, B., A combined reflectometry and quartz crystal microbalance with dissipation setup for surface interaction studies. *Review of Scientific Instruments* **2008,** *79* (7).
115. Rodenhausen, K. B.; Schubert, M., Virtual separation approach to study porous ultra-thin films by combined spectroscopic ellipsometry and quartz crystal microbalance methods. *Thin Solid Films* **2011,** *519* (9), 2772-2776.
116. Bailey, L. E.; Kambhampati, D.; Kanazawa, K. K.; Knoll, W.; Frank, C. W., Using surface plasmon resonance and the quartz crystal microbalance to monitor in situ the interfacial behavior of thin organic films. *Langmuir* **2002,** *18* (2), 479-489.
117. Domack, A.; Prucker, O.; Ruhe, J.; Johannsmann, D., Swelling of a polymer brush probed with a quartz crystal resonator. *Phys. Rev. E* **1997,** *56* (1), 680-689.
118. Bittrich, E.; Rodenhausen, K. B.; Eichhorn, K. J.; Hofmann, T.; Schubert, M.; Stamm, M.; Uhlmann, P., Protein adsorption on and swelling of polyelectrolyte brushes: A simultaneous ellipsometry-quartz crystal microbalance study. *Biointerphases* **2010,** *5* (4), 1-9.
119. Rodenhausen, K. B.; Duensing, B. A.; Kasputis, T.; Pannier, A. K.; Hofmann, T.; Schubert, M.; Tiwald, T. E.; Solinsky, M.; Wagner, M., In-situ monitoring of alkanethiol self-assembled monolayer chemisorption with combined spectroscopic ellipsometry and quartz crystal microbalance techniques. *Thin Solid Films* **2011,** *519* (9), 2817-2820.
120. Rodenhausen, K. B.; Guericke, M.; Sarkar, A.; Hofmann, T.; Ianno, N.; Schubert, M.; Tiwald, T. E.; Solinsky, M.; Wagner, M., Micelle-assisted bilayer formation of cetyltrimethylammonium bromide thin films studied with combinatorial spectroscopic ellipsometry and quartz crystal microbalance techniques. *Thin Solid Films* **2011,** *519* (9), 2821-2824.
121. Rodenhausen, K. B.; Kasputis, T.; Pannier, A. K.; Gerasimov, J. Y.; Lai, R. Y.; Solinsky, M.; Tiwald, T. E.; Wang, H.; Sarkar, A.; Hofmann, T.; Ianno, N.; Schubert, M., Combined optical and acoustical method for determination of thickness and porosity of transparent organic layers below the ultra-thin film limit. *Review of Scientific Instruments* **2011,** *82* (10).
122. Linse, P.; Wennerstrom, H., Adsorption versus aggregation. Particles and surface of the same material. *Soft Matter* **2012,** *8* (8), 2486-2493.